

STRATOSPHERIC SULFATE AEROSOL CLIMATE INTERVENTION IMPLICATIONS FOR
GLOBAL AGRICULTURE

By

BRENDAN JAMES CLARK

A dissertation submitted to the School of Graduate Studies

Rutgers, The State University of New Jersey

In partial fulfillment of the requirements for the degree of

Doctor of Philosophy

Graduate Program in Atmospheric Science

Written under the direction of Alan Robock and Lili Xia

And approved by

New Brunswick, New Jersey

January 2025

ABSTRACT OF THE DISSERTATION

Stratospheric Sulfate Aerosol Climate Intervention Implications for Global Agriculture

by BRENDAN JAMES CLARK

Dissertation Directors: Professors Alan Robock and Lili Xia

As the severity of climate change and its associated impacts continue to worsen, schemes for artificially cooling surface temperatures via planetary albedo modification are being studied. The method with the most attention in the literature is stratospheric sulfate aerosol climate intervention (SAI). Placing reflective aerosols in the stratosphere would have profound impacts on the entire Earth system, with potentially far-reaching societal impacts. This intervention strategy would impact crop production differently in different nations and would depend on the temperature target chosen. In this work, impacts on national maize, rice, soybean and wheat production were analyzed by looking at output from 11 different SAI scenarios carried out with a fully coupled Earth system model integrated with a crop model. Higher-latitude nations tend to produce the most calories under unabated climate change, while midlatitude nations maximize calories under moderate SAI implementation and equatorial nations produce the most calories from crops under high levels of SAI.

However, there is crop-model-related uncertainty as to how SAI would impact global agriculture. Here, three global gridded process-based crop models were forced by output of one SAI scenario to better understand the potential impacts on global maize productivity. Future SAI implementation relative to a climate change scenario benefits global maize productivity ranging between 0% and 11% depending on the crop model.

SAI would create an unprecedented climate where the relationship between surface temperatures and carbon dioxide concentrations are decoupled. The implications of this intervention for global crop protein concentrations have not yet been explored. Changes of global wheat, rice, soybean, and maize protein concentrations under climate change and sulfate aerosol climate intervention were simulated by global gridded crop models. Maintaining elevated CO₂ while reducing surface temperature increases with sulfate aerosol intervention would create small decreases to the protein concentrations of maize and rice, while wheat and soybean are minimally impacted. These decreases to protein under climate intervention partially offset any benefits to maize and rice yield.

ACKNOWLEDGEMENTS

This dissertation comprises work that has been previously published (Clark et al., 2023) or is in preparation to be published. Previously published works and works in preparation to be published are coauthored, but the primary contributions, lead authorship and original ideas to those works were that of this dissertation author.

DEDICATIONS

To my two advisors, Dr. Alan Robock and Dr. Lili Xia, whose advice, praise, and gentle criticism were vital to helping me become the curious and passionate scientist I am today.

To my loving family for their unwavering support throughout my entire educational career.

Table of Contents

Section 1.0: Introduction	1
Section 2.0: Methods	6
Section 2.1: Optimal climate intervention scenarios for crop production vary by nation	6
Section 2.2: Maize yield changes under sulfate aerosol climate intervention using three global gridded crop models	9
Section 2.3: Sulfate aerosol climate intervention could negatively impact the nutritional quality of maize and rice	12
Section 3.0: Results	14
Section 3.1: Optimal climate intervention scenarios for crop production vary by nation	14
Section 3.1.1: Solar constant reduction to represent SAI	14
Section 3.1.2: Crop production changes due to SAI.....	14
Section 3.1.3: Individual climate impacts on crop production under SAI	17
Section 3.2: Maize yield changes under sulfate aerosol climate intervention using three global gridded crop models	19
Section 3.2.1: Crop model comparison of maize production responses to SAI.....	19
Section 3.2.2: Crop model responses to changing diffuse radiation under SAI.....	21
Section 3.3: Sulfate aerosol climate intervention could negatively impact the nutritional quality of maize and rice	25
Section 3.3.1 Impacts to future crop protein under climate change and SAI	25
Section 3.3.2 Impacts to future crop yield and protein yield under climate change and SAI	26
Section 4.0: Discussion	29
Section 4.1: Optimal climate intervention scenarios for crop production vary by nation	29
Section 4.2: Maize yield changes under sulfate aerosol climate intervention using three global gridded crop models	31
Section 4.3 Stratospheric sulfate aerosol climate intervention could reduce the nutritional value of maize and rice	32
Section 5.0: Conclusions	35
Section 6.0: Data and code availability	39

Section 6.1: Optimal climate intervention scenarios for crop production vary by nation	39
Section 6.2: Maize yield changes under sulfate aerosol climate intervention using three global gridded crop models	39
Section 6.3 Stratospheric sulfate aerosol climate intervention could reduce the nutritional value of maize and rice	40
Section 7.0: References	41
Section 8.0: Table and Figures.....	46
Section 9.0: Supplementary Figures	65

Section 1.0: Introduction

As the severity of climate change and its associated impacts continue to intensify, schemes for artificially cooling surface temperatures via planetary albedo modification are being studied. The method with the most attention in the literature is stratospheric sulfate aerosol intervention (SAI). This climate intervention strategy aims to mimic volcanic eruptions by injecting sulfur dioxide into the stratosphere, where it oxidizes to form sulfuric acid, which then forms reflective aerosol particles (NAS, 2021). Injections would need to occur continuously to maintain decreased solar radiation and surface temperatures. These continued injections would have large impacts on the climate system, including temperature, precipitation, humidity and direct and diffuse radiation, which are controlling climate factors for crop production. These climate variables are all expected to change due to SAI.

Crops are grown to optimize their production in the current climate. Additional heat stress in the future is expected to reduce global yields of maize and push other crops such as wheat to higher latitudes (Jägermeyr et al., 2021). Limiting that additional heat stress with SAI could improve yields in the future and possibly maintain the present-day distribution of crop growth. This also means that SAI could decrease yields in higher-latitude nations relative to warming. Global carbon dioxide concentrations are anticipated to continue to grow, increasing the CO₂ fertilization effect and thus benefiting crops. C3 crops such as rice, soybean and wheat would benefit from increased CO₂ and reduced heat stress, since C3 crops tend to prefer cooler environments and their photosynthesis is limited by CO₂ (Farquhar et al., 1980). C4 plants such as maize are not as CO₂ limited, since they have an anatomical adaptation that allows them to increase the CO₂ concentration around the atmospherically isolated Rubisco enzyme, reducing photorespiration (Collatz et al, 1992). This means that increased CO₂ in the future would tend to

benefit C3 plants more than C4 plants. SAI would change regional precipitation patterns and humidity, potentially impacting regional crop production (Bala et al., 2008). It would also decrease total incoming solar radiation while increasing diffuse radiation due to scattering by the stratospheric aerosols, which would have opposing impacts on crop production (Proctor et al., 2018).

Previous modeling studies looking at SAI impacts on global agriculture have always used one crop model, either process-based or statistical and have produced diverse findings as those studies focus on different regions and crops under various SAI scenarios. One study used a statistical model including temperature, precipitation and CO₂ fertilization under a future SAI scenario to offset high-CO₂ warming (Pongratz et al., 2012). That study found a benefit to global rice, maize and wheat yields and a decrease in high-latitude rice. Another statistical study represented SAI based on volcanic eruptions to capture impacts on crops from changes to global sunlight (Proctor et al., 2018). They concluded that little of the global agricultural damage due to climate change would be offset by climate intervention, as the negative impacts from SAI on maize, rice, soybean and wheat due to changes in sunlight were balanced by benefits from global cooling. A few studies using dynamic crop models simulated regional agriculture responses to SAI, but the results vary depending on the SAI scenarios and the crop models used (Xia et al., 2014; Zhan et al., 2019). The next study used output from the Norwegian Earth System Model with prognostic biogeochemical cycling to run offline simulations of the Community Land Model version 5 (CLM5) to analyze impacts of SAI on maize, rice, soy, spring wheat, sugar cane and cotton¹⁷. They concluded that SAI used to reduce radiative forcing from RCP8.5 to RCP4.5 could benefit global yields by about 10% (Fan et al., 2021).

One previously unexplored topic is the idea that SAI implementation is not black and white, and there are a large variety of ways SAI could be done, including to reach several different global average temperature targets. How varying levels of SAI would impact regional crop production would be an important consideration for informing policy decision making. This work uses a fully coupled Earth system model with an interactive crop model to analyze the impacts on maize, rice, soybean and spring wheat production under multiple SAI scenarios that limit global average surface warming to targets set at the international negotiations at the 21st Conference of the Parties (COP21) in Paris of 1.5 °C and 2.0 °C above pre-industrial levels (Tilmes et al., 2020; Richter et al., 2022). Additional scenarios were used that go even further, reducing the global mean surface temperature increase to 1.0 °C and 0.5 °C above pre-industrial levels (MacMartin et al., 2022). These scenarios may be considered more policy-relevant than those previously studied, since they implement only moderate amounts of SAI to meet defined policy goals, rather than using large amounts of aerosols just to obtain a robust signal-to-noise ratio. This work also compares the impacts on crops of reducing incoming solar radiation through reducing the solar constant instead of SAI. Offline simulations were then conducted to understand which individual climatic changes caused by SAI influence impacts on crop production. Past studies have focused on global average crop impacts from a single SAI scenario or impacts on certain regions or individual nations. Since proposed SAI schemes so far have been based on controlling regional or global surface air temperatures, they would not also be able to control regional temperature, precipitation and other factors important to plants, so different nations would be impacted differently (Tilmes et al., 2018). This is particularly relevant considering that there may be many possible temperature targets that could be chosen for a SAI implementation.

In addition, all previous modeling studies assessing impacts to global agriculture have used just one crop model. It is important to compare impacts to global agriculture from the same SAI scenario across multiple crop models, as it has been shown that global process-based crop model responses to future climate change vary widely (Jägermeyr et al., 2021). Understanding the variation in crop model responses to SAI, including diffuse radiation fertilization, is valuable to reduce the uncertainties in crop responses to SAI. Communicating potential impacts and uncertainties of global agriculture from SAI is important for informing policymakers and ensuring knowledgeable decision making. This work uses three global process-based crop models: The Community Land Model version 5 crop model (CLMcrop), the Decision Support System for Agrotechnology Transfer global crop model (pDSSAT), and the Lund-Potsdam-Jena General Ecosystem Simulator crop model (LPJ-GUESS) to study maize yield change under the future climate warming scenario SSP2-4.5 and the Assessing Responses and Impacts of Solar climate intervention on the Earth system with stratospheric aerosol injection (ARISE-SAI; Richter et al., 2022). The climate forcing is from the Community Earth System Model version 2 (CESM2). This work aims to understand whether different crop models respond differently to a specific SAI implementation and highlight the importance of multi-crop model and multi-climate model assessment before drawing conclusions of SAI impacts on agriculture.

Previous studies that have assessed impacts to agriculture from SAI have focused primarily on crop yield or production, without considering changes to crop nutritional quality, such as crop protein content. An estimated 1.4 billion people will be at risk of protein deficiency by the year 2050, which is expected to be made worse by elevated carbon dioxide (CO₂) concentrations (Medek et al., 2017; Myers et al., 2014). Enhanced crop growth due to elevated CO₂ fertilization is associated with reduced concentrations of other elements, such as Nitrogen (Cotrufo et al., 1998;

Gifford et al., 2000), which is an indicator for crop protein content. There is evidence that elevated CO₂ concentrations have the potential to significantly reduce the protein content of major food crops, such as wheat and rice (Taub et al., 2008; Fernando et al., 2012; Myers et al., 2014; Chunwu et al., 2018). Elevated CO₂ reduces protein concentration in crop production by increasing carbohydrate accumulation through CO₂ fertilization, which dilutes crop nitrogen content, and by inhibiting nitrate assimilation, limits the nitrogen available for protein synthesis (Myers et al., 2014; Taub et al., 2007). Furthermore, elevated CO₂ reduces the nitrogen-rich enzyme Rubisco, which further lowers nitrogen and protein levels in key crops like wheat and rice (Bloom et al., 2010)

While the impact of rising temperatures on crop nutritional quality is less understood, there is growing evidence that this could have a positive impact on crop nutritional quality, potentially helping to counteract some of the negative effects of rising CO₂ (Wang et al., 2019; Köhler et al., 2019; Guo et al., 2022). Field experiments found that with a 1.2°C – 2.5°C warming relative to the average temperature during the late 20th century, nitrogen and protein concentrations may increase in crops by enhancing nitrogen uptake and translocation through increased transpiration, as well as by accelerating nitrogen mineralization and plant metabolic rates (Yin et al., 2021; Wang et al., 2018). However, with extreme high temperature, nitrogen and protein concentration can be reduced as the heat stress diminishes nitrogen assimilation (Ainsworth & Rogers, 2007). Since SAI would reduce surface temperature increases while maintaining elevated CO₂, it has the potential to further reduce crop nutritional quality below what may occur with climate change alone.

Section 2.0: Methods

Section 2.1: Optimal climate intervention scenarios for crop production vary by nation

The climate change and climate intervention scenarios were simulated using the Community Earth System Model version 2 Whole Atmosphere Community Climate Model Version 6 CESM2(WACCM6) with troposphere, stratosphere, mesosphere and lower thermosphere chemistry, and CLM5 with coupled CLM-5crop (Danabasoglu et al., 2020; Lombardozzi et al., 2020). CESM2 is currently the only Earth system model with a built-in coupled crop model, making it ideal for analyzing impacts on crops under future climates. WACCM6 has a resolution of $0.95^\circ \times 1.25^\circ$ latitude–longitude with 70 vertical layers, reaching 150 km above sea level (Tilmes et al., 2020; Gettelman et al., 2019). WACCM6 uses the updated four-mode version of the Modal Aerosol Module version 4 to represent tropospheric and stratospheric aerosol dynamics (Liu et al., 2016).

WACCM6 and other model components were coupled to CLM5 and CLM5crop. CLM5crop currently simulates only maize, rice, soybean, spring wheat, sugar cane and cotton. Focus was put on maize, rice, soybean and spring wheat as those four crops comprise most of the global food production as well as caloric consumption (FAO, 2022). Land unit grid cells within CLM5 can be partitioned to include prescribed transient crop area when CLM5crop is active. Crops are planted and then transition through leaf emergence, grain fill and harvest phases (Lombardozzi et al., 2020). To calculate yield, grain carbon is assumed to be 45% of the total dry weight, and a harvest efficiency of 85% is assumed for all crops (Lombardozzi et al., 2020). The coupling between crops, the land surface and the atmosphere allows for the direct analysis of potential impacts on crops from changes in temperature, precipitation, CO₂, humidity and diffuse and direct radiation. Crop production was calculated using fully coupled CESM2–CLM5crop yield

output and time-varying cropping area from the accompanying SSP scenarios. To determine how SAI would impact food production, yield output was converted to calories. Food caloric production is defined here as follows: Production (kilocalories per year) = Yield (tonnes per hectare per year) × Cropping Area (hectares) × Crop Nutritional Value (kilocalories per tonne) (FAO, 2022).

Reference CMIP6 climate change scenarios SSP2-4.5, SSP5-3.4-OS and SSP5-8.5 (O'Neill et al., 2016) were simulated with accompanying climate intervention scenarios to limit anthropogenic warming to 0.5, 1.0, 1.5 or 2.0°C above pre-industrial levels. Different SSPs have varying amounts of nitrogen fertilizer application and land-use change. SSP2-4.5 is a medium-emission scenario, with the CO₂ concentration starting at 415 ppm in 2020 and increasing to 600 ppm by 2100 (O'Neill et al., 2016). SSP5-8.5 is an unmitigated high-emission scenario, with the CO₂ concentration growing rapidly throughout the twenty-first century from 415 ppm in 2020 to 1,100 ppm in 2100 (Gettelman et al., 2019). SSP5-3.4-OS starts in 2015 and goes to 2100; it follows SSP5-8.5 until 2040, and thereafter strong mitigation efforts (such as carbon dioxide removal) are implemented (O'Neill et al., 2016). Even with strong mitigation and negative emissions starting in 2040, the CO₂ concentration still grows until 2065, when it reaches its peak of about 525 ppm (Figure 1). All three climate change scenarios see an overshooting of both global average temperature targets set at COP21 of 1.5°C and 2.0°C above pre-industrial levels. Temperatures above these targets have been deemed to have significant negative impacts on societies and ecosystems (IPCC, 2021).

To simulate SAI, a feedback controller algorithm is used to calculate the amount of SO₂ injected into the stratosphere each year at 15°N, 15°S, 30°N and 30°S. This calculation is made every year depending on the previous year's global mean temperature, interhemispheric temperature gradient and equator-to-pole temperature gradient (Kravitz et al., 2017). A more in-

depth exploration of the SAI strategies considered is available in accompanying papers (Tilmes et al., 2020; Richter et al., 2022; MacMartin et al., 2022). Scenarios following SSP5-3.4-OS use SAI to limit global mean warming to both COP21 targets of 1.5°C and 2.0°C above pre-industrial levels (Tilmes et al, 2020). The scenario SSP2-4.5-1.5°C limits warming to 1.5°C under SSP2-4.5 and is named Assessing Responses and Impacts of Solar Climate Intervention on the Earth System with Stratospheric Aerosol Injection (ARISE-SAI-1.5) (Richter et al., 2022). SSP2-4.5-1.0°C and SSP2-4.5-0.5°C reduce the global mean temperature increase to 0.5°C and 1.0°C above pre-industrial levels, below the warming targets set at COP21 (MacMartin et al., 2022). SSP2-4.5-1.0°C and SSP2-4.5-0.5°C were carried out with a simpler version of CESM2(WACCM6): one containing interactive chemistry only in the middle atmosphere and not in the troposphere. This is not expected to impact crop results, as the two versions show almost identical responses to large stratospheric aerosol loads (Davis et al., 2023). These simulations start SAI in the year 2035. There is also a scenario that follows SSP5-8.5 and uses SAI to maintain temperatures of 1.5°C above pre-industrial levels (Tilmes et al., 2022). In this scenario, climate intervention begins in the year 2020. Additional simulations used in this study were run as part of the Geoengineering Model Intercomparison Project Phase 6 (Kravitz et al., 2015). These include G6Sulfur and G6Solar. G6Sulfur uses SO₂ injections to bring global mean temperatures from the high-emission climate change scenario SSP5-8.5 down to the medium-emission scenario SSP2-4.5, and G6Solar uses solar dimming to achieve the same temperature reduction (Visioni et al., 2021).

Section 2.2: Maize yield changes under sulfate aerosol climate intervention using three global gridded crop models

In this analysis the atmospheric forcing used to force the global crop models is from the CESM2 (Danabasoglu et al., 2020) using the WACCM6 configuration. The background climate change scenario followed the Shared Socioeconomic Pathway (SSP) 2, with Representative Concentration Pathway 4.5, hereafter SSP2-4.5 (Meinshausen et al., 2020). This analysis also uses the ARISE-SAI scenario (Richter et al., 2022). SO₂ is injected every year within the model into one grid box at about 21.5 km height at four different latitudes: 30°N, 15°N, 15°S, and 30°S. The location and amount of SO₂ injection is determined through a feedback control algorithm that attempts to maintain three objectives simultaneously: global mean temperature the same as during 2020-2039, which in this model is 1.5°C above preindustrial, the interhemispheric temperature gradient during 2020-2039, and the equator-to-pole temperature gradient during 2020-2039. SAI starts in the year 2035, and the years 2016-2025 of SSP2-4.5 were used as a reference period. Additional details on the climate model simulations can be found in Richter et al. (2022).

To understand impacts to global maize productivity under both climate change and SAI scenarios, three different well-developed global process-based crop models were used: version 5 of the CLM crop model (CLM5crop), LPJ-GUESS, and pDSSAT v4.8.0 (Lawrence et al., 2019; Lindeskog et al., 2013; Hoogenboom et al., 2019; Elliott et al. 2014). One ensemble member each from the CESM2(WACCM6) simulations of SSP2-4.5 (2016-2068) and SSP2-4.5 with SAI (2036-2068) were chosen to force the three crop models, with 2016-2025 of SSP2-4.5 serving as the reference period. The climate model forcing was downscaled to 0.5° by 0.5° longitude-latitude resolution. LPJ-GUESS and pDSSAT are forced by daily atmospheric inputs, while CLM5crop was run with 3-hourly and 1-hourly data. Crop model simulations followed transient CO₂

concentrations following SSP2-4.5 (Meinshausen et al., 2020). Other inputs such as planting dates, cropping area, nitrogen fertilizer application, and atmospheric NO₃ and NH₄ deposition were held constant at 2015 levels following the Global Gridded Crop Model Intercomparison phase 3 protocol (Jägermeyr et al., 2021). This means that all impacts to maize production are driven solely by changes to the climate. All crop models simulate maize under both rainfed and fully irrigated conditions.

While LPJ-GUESS is not able to partition between direct and diffuse radiation, CLM5crop and pDSSAT had additional simulations that isolated the impact of enhanced diffuse radiation fertilization under SAI. pDSSAT ran the climate change and SAI scenarios with either prescribing total incoming shortwave solar radiation (default) or a novel partitioning between direct and diffuse shortwave radiation. Since the pDSSAT CERES-Maize model calculates daily photosynthesis using radiation use efficiency (RUE) (Jones and Kiniry, 1986), the partitioning between direct and diffuse radiation is based on the fractional change in RUE as a function of the diffuse fraction (DF) detailed in Greenwald et al. (2006). This approach is like the DSSAT NWheat diffuse radiation response (Yang et al., 2013) and the pDSSAT diffuse radiation response from Shiferl et al. (2018). A maximum change in RUE of 50% at DF of 0.8 is used to prevent overestimation of plant growth (Greenwald et al., 2006). The diffuse fraction is calculated as:

$$DF = \frac{SDIF}{SRAD} \quad (1)$$

where SDIF is the daily diffuse shortwave solar radiation (MJ m⁻²) and SRAD is the daily total incoming shortwave solar radiation (MJ m⁻²) provided from CESM2. The fractional change in RUE with a maximum change of 50% is calculated as:

$$RUE_{dif} = RUE * (1 + (1.21 * DF^3 - 3.26 * DF^2 + 2.92 * DF - 0.37)) \quad (2)$$

where RUE_{dif} is the daily RUE with diffuse radiation effect (g MJ^{-1}), RUE is the default maize-specific parameter (g MJ^{-1}), and the constants are from Greenwald et al. (2006). Daily potential dry matter production (PCARB, g) is then calculated via:

$$PCARB = IPAR * RUE_{dif} * PCO2 \quad (3)$$

where IPAR is the daily intercepted photosynthetically active radiation (MJ) and PCO_2 is the crop-specific CO_2 effect on growth rate (Jones and Kiniry, 1986). If SDIF is not provided, the model uses the default RUE processes.

CLM5crop ran simulations that tested the impact of changing the direct/diffuse ratio under SAI relative to climate change. This was done by first reducing the total solar radiation of SSP2-4.5 to equal that of ARISE-SAI. Then the direct and diffuse radiation of SSP2-4.5 was replaced by the direct and diffuse radiation of ARISE-SAI. This allows the impact of just changing the direct/diffuse ratio under SAI to be understood while ignoring changes to total solar radiation. These additional radiation-partitioned scenarios allow the impact of diffuse radiation fertilization on global maize production under SAI to be tested in these two models.

Section 2.3: Sulfate aerosol climate intervention could negatively impact the nutritional quality of maize and rice

The atmosphere data used for this analysis is the same as that which is described in Section 2.2 and follows SSP2-4.5 and ARISE-SAI. The crop models have interactive carbon and nitrogen cycling, and output grain level carbon and nitrogen storage levels upon harvest. All three crop models were harmonized following the Global Gridded Crop Model Intercomparison Phase 3 protocol, whereby planting dates, cropping areas, nitrogen fertilizer application, and atmospheric NO_3 and NH_4 deposition were held constant at 2015 levels throughout the simulations (Jägermeyr et al., 2021). One ensemble member from the output of CESM2(WACCM6) of SSP2-4.5 and ARISE-SAI was chosen as climate forcing for the crop models. The atmospheric forcing data were downscaled to 0.5° by 0.5° longitude-latitude resolution. LPJ-GUESS and pDSSAT are forced by daily inputs, while CLMcrop was run with 3-hourly and 1-hourly atmosphere data. CLMcrop and LPJ-GUESS simulated maize, wheat, rice, and soybean, while pDSSAT only simulated maize. Due to harmonization of all other inputs, the impacts to crop protein are due entirely by changes to the climate under future climate change and SAI. Crop protein content was estimated using the grain N:C ratio, and protein yield was then calculated by multiplying grain yield by grain protein concentration.

Crop yields for all three crop models have been previously calibrated and validated against the historical period. CLMcrop, LPJ-GUESS, and pDSSAT all showed a significant positive correlation with simulated interannual global maize yield when compared to observations (Müller et al., 2017; Clark et al., 2023). CLMcrop and LPJ-GUESS also showed significant positive correlation to observations of global wheat and rice yields (Müller et al., 2017; Clark et al., 2023). However, CLMcrop and LPJ-GUESS were not able to significantly replicate the interannual yield

variability of soybean, making future projections of soybean for these models less reliable (Müller et al., 2017; Clark et al., 2023).

There are no global datasets of observations of crop protein, making validating the crop models for their ability to simulate protein content challenging. To validate the ability of crop model simulated grain C/N to respond to future climates, simulations of CLMcrop with ambient CO₂ (370 ppm) compared with elevated CO₂ (570 ppm) were evaluated against the results of free-air CO₂ enrichment (FACE) experiments from Myers et al. (2014). Supplementary Figure 1 shows that CLMcrop did a reasonable job capturing protein responses to elevated CO₂ for maize, rice, soybean, and wheat. Myers et al. (2014) found a decrease to protein of wheat and rice under elevated CO₂, with minimal impact on maize and soybean, which is consistent with the results from CLMcrop (Supplementary Figure 1). Experiments from Myers et al. (2014) took place during the years 2007-2010 for wheat, 2007-2010 for rice, 2001-2008 for soybean, and 2008 for maize. The evaluation period used for CLM5crop are from years 2016-2020. Temperature differences between our simulations and results from Myers et al. (2014) could cause results to be slightly different.

Section 3.0: Results

Section 3.1: Optimal climate intervention scenarios for crop production vary by nation

Section 3.1.1: Solar constant reduction to represent SAI

Previous studies of crop and vegetation impacts from SAI have used solar constant reduction to represent impacts from SAI (Xia et al., 2014; Dagon et al., 2019). The Geo-engineering Model Intercomparison Project Phase 6 experiments use both solar constant reduction (G6Solar) and sulfate aerosol intervention (G6Sulfur) to limit radiative forcing from Shared Socioeconomic Pathway scenario SSP5-8.5 down to what it would be with SSP2-4.5 (Kravitz et al., 2015). These two scenarios result in similar temperature, precipitation, humidity and total solar radiation responses over all cropland area globally (Figure 1). Although most yield responses to these climate forcings are not significantly different between the G6 experiments, there is a slight benefit to yields under G6Sulfur compared with G6Solar (Supplementary Figure 2). Increased crop yields under G6Sulfur are expected due to the increased scattering of solar radiation by the sulfate aerosols, enhancing downward diffuse solar radiation in the G6Sulfur experiment relative to G6Solar (Figure 1f). This enhanced diffuse radiation increases yields for maize, rice, soybean and spring wheat in G6Sulfur compared with G6Solar. Previous studies that used solar constant reduction to simulate SAI, or that used a crop model that did not partition between direct and diffuse radiation, could thus have underestimated crop yield responses to SAI.

Section 3.1.2: Crop production changes due to SAI

Limiting anthropogenic warming increases the global sum of calories from maize, rice, soybean and spring wheat under all SAI scenarios (Figure 2). Under the scenario SSP5-8.5-1.5°C, the number of global calories from the four crops simulated increases by $22 \pm 1\%$ relative to SSP5-

8.5 during the years 2060–2069 (Figure 2a). Total global calories during the years 2060–2069 increase by 24% under SSP2-4.5-0.5°C, 20 ± 1% under SSP2-4.5-1.0°C, 12 ± 3% under SSP2-4.5-1.5°C, 18% under SSP5-3.4-1.5 °C, 12 ± 1% under SSP5-3.4-2.0°C, 16 ± 1% under G6Solar and 19 ± 1% under G6Sulfur (Figure 2a). These changes to caloric production under climate intervention are all beyond the standard deviation of the 50-year historical period of ±5% (Figure 2a). How much total calories increase depends on the time period and therefore the CO₂ concentration and the amount of SAI (Figure 2).

While global caloric production shows benefits under SAI, there are also many regions and nations where production will be reduced from SAI relative to warming without SAI. Maize, rice, soybean and spring wheat yields are anticipated to increase in high latitudes from warming due to climate change (Jaegermeyr et al., 2021). Some of the world's largest crop producers are in high-latitude regions (Figure 3). Reducing warming with stratospheric aerosols tends to decrease production in these high-latitude nations relative to a warming scenario (Figures 3–6). Comparing the magnitude of calories produced under a given scenario must be done between scenarios that share the same SSP, since different SSPs have varying amounts of nitrogen fertilizer application, cropping area and CO₂ concentration (Figure 1 and Supplementary Figure 4). Canada produces the most calories under the climate change scenario SSP2-4.5 (Figure 4). Russia produces the most calories under the high-emission scenario SSP5-8.5 (Figure 5) and climate change scenario SSP5-3.4-OS (Figure 6). Midlatitude nations tend to prefer more moderate amounts of SAI to maximize crop calories (Figures 4–6). Other, lower-latitude nations benefit from larger amounts of SAI, showing the most calories from crop production when temperatures are limited the most, such as in SSP2-4.5-0.5°C (Figure 4). Most the world's top crop-producing nations show increases in their production under SAI, but each SAI scenario has multiple top producing nations with decreases in

their production relative to climate change (Figure 3). None of the 11 climate change or climate intervention scenarios analyzed here benefit everyone. Although global production tends to increase with more SAI, the number of nations that show a decrease in their production does also (Supplementary Figure 5). Under SSP2-4.5, total calories from maize, rice, soybean and spring wheat are the highest in 102, 31 and 21 nations when maintaining temperatures that are 0.5, 1.0 and 1.5°C above pre-industrial levels with SAI during the years 2060–2069, respectively (Figure 4). There are 12 nations that maximize calories from crops under the unabated climate change scenario SSP2-4.5 during the years 2060–2069 (Figure 4). Even if 102 nations would produce the most calories from limiting temperatures to 0.5 °C above pre-industrial levels under SSP2-4.5 using SAI, there would still be 64 nations that would not, including the 12 that may not benefit at all from SAI. Under SSP5-8.5, 121 nations produce the most calories under SSP5-8.5-1.5°C, 20 under G6Sulfur, 9 under G6Solar and 18 others produce the most calories from crops under the high-emission scenario SSP5-8.5 during the years 2060–2069 (Figure 5). Under SSP5-3.4-OS, 89 nations produce the most calories from maize, rice, soybean and spring wheat under the scenario SSP5-3.4-1.5°C, 56 nations under SSP5-3.4-2.0°C and 22 nations under SSP5-3.4-OS (Figure 6). The number of nations that maximize their calories under a specific temperature target varies by crop (Figures 4–6). Calories from rice are greater in more nations under climate change relative to those from other crops (Figures 4–6). Soybean calories tend to be largest in more nations when temperatures are limited the most with climate intervention compared with other crops (Figures 4–6). This is due to the respective low and high temperature sensitivity of rice and soybean (Figure 7). Most of the world's top crop-producing nations increase production under climate intervention (Figure 3). Although most nations would produce the most total calories from crops under the more

extreme SAI scenarios, there are still many countries that would not, potentially causing conflict (Supplementary Figure 5).

Section 3.1.3: Individual climate impacts on crop production under SAI

To understand why crop production is changing under SAI, offline simulations of CLM5crop were run that only allowed single climate variables to change due to climate intervention. The individual contributions to crop production impacts from changing temperature, precipitation, specific humidity, total solar radiation and diffuse radiation were tested separately under SAI used to maintain warming of 1.5°C above pre-industrial levels under SSP2-4.5. The period 2060–2069 under these scenarios also represents 1°C of global temperature reduction using SAI. Increased CO₂ fertilization has a large benefit to crop production under SSP2-4.5 and SSP5-8.5 during the years 2060–2069 (Supplementary Figure 3). CO₂ concentrations in SSP5-3.4-OS increase slightly and then begin to decrease over the years 2060–2069, with a small overall benefit to crop production (Figure 1 and Supplementary Figure 3). CO₂ concentrations are prescribed and do not change under climate intervention, relative to climate change, in the model used in this study, so these changes are not due to SAI. This high sensitivity to CO₂ means that changes to maize, rice, soybean and spring wheat production under SAI in the future would still be an increase relative to present-day conditions for most nations (Supplementary Figure 6). Changes to precipitation, humidity, total radiation and diffuse radiation had minimal impacts on global maize, rice, soybean and spring wheat production relative to temperature (Figure 7). However, there are regional changes to these variables that may become important. Precipitation changes had a significant negative impact on midlatitude maize and spring wheat (Supplementary Figure 8). Under SSP2-4.5-1.5°C, aerosols are injected primarily in the Southern Hemisphere, meaning that impacts on Northern Hemisphere crops from increased diffuse radiation or decreased total

radiation may be subdued (Richter et al., 2022). Limiting warming under climate intervention had the most areas with a significant impact on yield for all crops compared with changes to other climate variables (Supplementary Figures 7–11). Total solar radiation reduction under SSP2-4.5-1.5°C had the least significant impact on crop production, showing almost no areas of statistically significant yield reductions relative to SSP2-4.5 (Supplementary Figure 21) compared with regional yield responses to other climate variables (Supplementary Figures 7–11). These results will depend on the amount of SAI implemented, the scenario and time period analyzed, and the crop model being used.

Section 3.2: Maize yield changes under sulfate aerosol climate intervention using three global gridded crop models

Section 3.2.1: Crop model comparison of maize production responses to SAI

Figure 8 shows the annual time series of global maize production change under both climate change scenario SSP2-4.5 and climate change with SAI implemented to maintain 1.5°C above preindustrial levels (SSP2-4.5-SAI-1.5C) relative to the reference period (2016-2025). CLM5crop and pDSSAT show very similar responses to interannual variability of production under climate change scenario SSP2-4.5 (Figure 8). CLM5crop and pDSSAT show a decrease in maize production over time under SSP2-4.5 relative to the reference period, while LPJ-GUESS shows almost no trend (Figure 8). The response to SAI varies between models. Compared with SSP2-4.5, CLM5crop and pDSSAT show a benefit to production of 4% and 11% under SAI over the years 2049-2068, while LPJ-GUESS shows a difference in global production of 0% between the two scenarios during the same time period (Figures 8 and 9). In CLM5crop, this increase to production under SAI causes the global production of maize to increase relative to the reference period, while in pDSSAT the change to global production under SAI is still a decrease of about 10% relative to the reference period (Figure 9). LPJ-GUESS exhibits a stronger response to elevated atmospheric CO₂ concentrations and a weaker sensitivity to higher temperature resulting in positive yield changes under climate change, relative to other crop models like pDSSAT that show substantial declines in maize productivity (Jägermeyr et al., 2021; Müller et al., 2024). These models differ in process representation. For example, CLM5crop and LPJ-GUESS do not have mechanisms in place to accelerate crop senescence from extreme heat; heat stress is simulated in these models by only reducing photosynthesis and water use efficiency (Lawrence et al., 2019; Lindeskog et al., 2013). In addition to photosynthesis and drought stress, pDSSAT uses heat stress

damage functions that accelerate crop senescence above certain temperature thresholds (Hoogenboom et al., 2019; Elliott et al. 2014). This means that impacts from extreme temperature would tend to be stronger under both future climate change and SAI in pDSSAT when compared to CLM5crop and LPJ-GUESS, resulting in exacerbated global production impacts in pDSSAT (Figures 8, 9, and 10). pDSSAT also has one of the largest negative responses to future climate change in a recent study on future production impacts from 12 global gridded crop models (Jägermeyr et al, 2021), while LPJmL (a branched-off version using similar roots as LPJ-GUESS) had one of the smallest responses to future maize production, which is consistent with our findings (Figure 10). The changes to global maize production in CLM5crop and LPJ-GUESS under both climate change and SAI still mostly fall within one standard deviation of interannual variability in the reference period and are, therefore, not as significant as changes in pDSSAT (Figure 8). LPJ-GUESS lacks partitioning between direct and diffuse radiation, so there is no impact of enhanced diffuse radiation fertilization under SAI, which has been shown to play a role in global crop responses to SAI in process-based and statistical crop models (Proctor et al., 2018; Fan et al., 2021; Clark et al., 2023).

CLM5crop and pDSSAT both show that SAI benefits maize yield relative to climate change in nearly all areas of the world (Figure 10). While there are some regions where maize yield decreases in CLM5crop, such as parts of the United States and Russia, these decreases are not statistically significant (Figure 10). All significant changes to yield in CLM5crop and pDSSAT tend to be positive (Figure 10). LPJ-GUESS has essentially no significant changes to yield under SAI relative to climate change, which contrasts the results for CLM5crop and pDSSAT (Figure 10). This is likely due to the three models having varying sensitivity to temperature, with pDSSAT having the strongest sensitivity, CLM5crop having a moderate sensitivity, and LPJ-GUESS having

a weak sensitivity (Clark et al., 2023; Müller et al., 2024). The importance of individual climate forcings under SAI was tested in CLMcrop in Clark et al. (2023), where temperature reduction under SAI was found to be the largest contributor to maize production changes. It is also possible that the reduction in total solar radiation under SAI negates any benefits from cooling in LPJ-GUESS, as LPJ-GUESS does not simulate diffuse radiation fertilization.

Although global maize production increases under SAI relative to climate change in pDSSAT, the changes under SAI are still a decrease of around 10% relative to the reference period over the years 2049-2068 (Figure 9). SAI would help to minimize the reduction in maize yield under SSP2-4.5 in CLM5crop and pDSSAT. LPJ-GUESS shows similar global production responses under both SAI and climate change (Figure 9). Crop models introduce greater uncertainty than climate models when estimating future agriculture yield due to their varying sensitivities to temperature, precipitation, and CO₂ concentration (Jägermeyr et al., 2021). This uncertainty remains true with SAI as well, with the three crop models used here showing a range of responses to future maize yield under both climate change and SAI. Since SAI would create an unprecedented environment for crops, existing crop models might not fully capture impacts from specific changes induced by SAI. Nevertheless, as a preliminary step, it is essential to simulate SAI's impact on agriculture using crop models, and this study serves as a pilot for a more comprehensive multi-crop, multi-climate model assessment.

Section 3.2.2: Crop model responses to changing diffuse radiation under SAI

One of the key unique environmental changes resulting from SAI would be the modification of the quantity and partitioning of radiation reaching Earth's surface. SAI would reduce total incoming solar radiation and direct radiation, while increasing the fraction of diffuse light due to the scattering effect of the sulfate aerosols and changing cloud coverage. Decreasing

total solar radiation tends to decrease plant photosynthesis, while increasing the diffuse fraction tends to increase photosynthesis by allowing more sunlight to reach leaves that are normally shaded (Roderick et al., 2003). This response has also been observed during volcanic eruptions, which are an analog for what could be expected from SAI (Gu et al., 2003).

It is not entirely clear which of these opposing mechanisms would dominate in the crop yield response. Proctor et al. (2018) used an empirical yield model based on observations of the 1991 Mount Pinatubo eruption to assess how SAI might impact global yield. They found an overall negative effect from the sulfate aerosols' impact on total radiation that roughly balanced benefits from cooling. However, the aerosols from the Pinatubo eruption were found to be more backscattering than that of other eruptions, such as El Chichón, and this backscattering is not necessarily seen in climate model simulations of SAI (Proctor et al., 2018). Proctor et al. (2018) also did not separate the effects of changing surface ozone and ultraviolet radiation, which could confound the results and make drawing comparisons more difficult, as current crop models do not account for changing surface ozone and ultraviolet radiation. Previous crop modeling studies of diffuse radiation impacts under SAI have tended to find positive impacts from enhanced diffuse radiation fertilization with negative impacts from reducing total solar radiation, with the overall effect being small (Fan et al., 2021; Clark et al., 2023). However, these studies used just one crop model and were forced by different scenarios. This variation in results between empirical and modeling studies means that further analysis with additional crop models is needed. Impacts to maize from diffuse radiation fertilization under SAI using CLM5crop and pDSSAT were tested (since LPJ-GUESS only considers total radiation).

Figure 11 shows the impact from diffuse radiation fertilization under SAI on global maize production in pDSSAT and CLM5crop. For pDSSAT, this is calculated by comparing the

differences between the SAI and climate change scenario with diffuse radiation input data included and excluded. CLM5crop ran simulations that compared the impact of changing the ratio of direct to diffuse radiation under SAI compared with the direct to diffuse ratio under climate change. Under the ARISE-SAI scenario, the feedback control algorithm used to determine the amount and location of SO₂ injection places the majority of SO₂ injection in the Southern Hemisphere at 15°S (Richter et al., 2022), resulting in the enhancement of diffuse radiation from the injected aerosols being concentrated in the Southern Hemisphere (Figure 12). Since most maize is grown in the Northern Hemisphere, the impacts from diffuse radiation fertilization on global maize are muted under this scenario with the production changes within the range of natural variability seen in the reference period (Figures 1 and 6). There are even some years where production goes down from changing diffuse radiation, but this is likely due to cloud-related weather, natural climate variability, or changes in anthropogenic emissions of aerosols under the scenario SSP2-4.5 (Figures 4 and 5). This could be reduced in future studies by using additional ensemble members. Impacts to global maize production from diffuse radiation are small in both CLM5crop and pDSSAT, and vary between about -3% and +3%, with regional variations (Figure 11). In addition to most of the SO₂ injection taking place in the Southern Hemisphere, this SAI scenario also has a small temperature signal relative to other scenarios, like those used in Proctor et al. (2018) and Fan et al. (2021), as the SO₂ injection amount is small relative to these previous studies (Richter et al., 2022). This work relies on one climate model ensemble member to assess impacts from diffuse radiation, which is subject to substantial noise due to cloud-related weather. Most impacts to maize yield from diffuse radiation occurring in the Northern Hemisphere are subject to this noise, and the largest responses to yield are in the Southern Hemisphere where there are the largest changes to diffuse radiation (Figures 4 and 5). Other climate models simulating the same SAI scenario with

different SO₂ injection locations and amounts may show different diffuse radiation effects on crops (Henry et al., 2023). Using additional climate models and crop models forced by different scenarios would help to reduce uncertainties.

Section 3.3: Sulfate aerosol climate intervention could negatively impact the nutritional quality of maize and rice

Section 3.3.1 Impacts to future crop protein under climate change and SAI

Under global warming, protein contents in maize and soybean increase in CLM5crop and pDSSAT, with no significant change observed in wheat and rice, likely due to the balance between the negative effects of elevated CO₂ and the positive impacts of warming (Figure 13). In contrast, LPJ-GUESS shows a decreasing trend in protein content across all four crops. Both CLMcrop and LPJ-GUESS show a decreasing trend of protein content for wheat and rice in both scenarios due to increasing CO₂ fertilization causing a “dilution” effect to protein for these crops (Figure 13). This trend is not seen for maize as it is a C₄ crop and therefore has a mechanism to increase the concentration of CO₂ at the Rubisco enzyme sight, decreasing its susceptibility to CO₂ fertilization (Collatz et al., 1992). Soybean is a C₃ crop and therefore its photosynthesis is limited by CO₂, like wheat and rice, increasing its CO₂ fertilization and possible protein dilution (Farquhar et al., 1980). While there is a small deceasing trend in soybean protein content in LPJ-GUESS, this is not seen in CLMcrop (Figure 13). This may be explained by the ability for legumes such as soybean to use extra carbon gained from CO₂ fertilization for Nitrogen fixation, balancing their grain C:N ratio (Ainsworth et al., 2020).

Figure 13 shows the time series of changes to global average crop protein for maize, wheat, rice, and soybean under SSP2-4.5 and ARISE-SAI relative to the reference period. LPJ-GUESS shows a decreasing trend in protein content across all four crops. Towards the end of the simulations, global average maize protein content decreases by approximately 10% in CLM5crop and 5% in pDSSAT under SAI relative to climate change (Figure 13). There are also decreases to global rice protein of about 5% under SAI relative to climate change in CLMcrop throughout the

simulations (Figure 13). There is a small decrease to wheat protein content in CLMcrop under SAI towards the end of the simulations relative to SSP2-4.5 (Figure 13). LPJ-GUESS shows very small differences to protein content in four crops under SAI and climate change (Figure 13).

Section 3.3.2 Impacts to future crop yield and protein yield under climate change and SAI

While most crop modeling studies have focused on projections of future crop yield, incorporating results from changes to protein allows for projections of protein yield under future climates to be made. Figure 14 shows changes to both global average yields and protein yields under SAI and climate change for maize, wheat, rice, and soybean. In CLMcrop there is a decrease to maize yield under SSP2-4.5, with an increase to maize yield under ARISE-SAI relative to the reference period (Figure 14). However, the protein yields for maize in CLMcrop are very similar under SSP2-4.5 and ARISE-SAI relative to the reference period (Figure 14), as cooling from ARISE-SAI decreases maize protein concentration in CLMcrop relative to the reference period (Figure 14). pDSSAT shows much larger decreases of maize yield under SSP2-4.5, while SAI makes changes to maize yield back to the level of the reference period (Figure 14). Maize protein yield in pDSSAT shows a slightly smaller difference between the SSP2-4.5 and ARISE-SAI scenarios but ARISE-SAI still increases maize protein yield significantly mainly due to the increasing of maize yield (Figure 14). Wheat, rice, and soybean show increasing trends to global average yield in both SSP2-4.5 and ARISE-SAI relative to the reference period due to increasing CO₂ fertilization throughout the simulations (Figure 14). This increasing CO₂ fertilization for these C₃ crops is accompanied by decreases to protein concentrations for wheat and rice in CLMcrop and LPJ-GUESS (Figure 14). Therefore, even with an increasing trend of rice and wheat yields under SSP2-4.5, their protein yields show less increases. In addition, cooling from SAI further reduces protein yields in rice and wheat (Figure 14). Since soybean is a leguminous crop and does

not see large reductions to protein in CLMcrop or LPJ-GUESS, the impacts to future yield and protein yield are largely similar (Figure 14).

Figure 15 shows how accounting for crop protein impacts the changes to global crop yields under SAI relative to climate change. In the crop models used, all four crops tend to show increases to global yields under SAI relative to climate change (Figure 15). For maize, there is a large benefit to global yields in pDSSAT under SAI, a moderate benefit in CLMcrop, and very small changes to maize yields in LPJ-GUESS relative to SSP2-4.5. Comparing changes to maize yields under SAI to protein yields, protein yields cause benefits under SAI to be decreased slightly in pDSSAT (Figure 15). In CLMcrop, impacts to global maize from SAI go from being positive, with yields increasing by up to 10% relative to climate change, to being negligible once protein changes are also considered (Figure 15). Impacts to rice are also worsened under SAI when looking at protein yield instead of just yield (Figure 15). In CLMcrop, impacts to rice go from being mostly negligible to a decrease under SAI relative to climate change once protein changes are included (Figure 15). LPJ-GUESS shows very little differences between yield and protein yield for all four crops, while CLMcrop shows little differences between yield and protein yield for wheat and soybean (Figure 15).

Figure 16 shows the regional impacts to yield and protein yield under future climate change relative to the reference period. Accounting for protein causes there to be larger decreases to yield of maize in parts of Europe and Africa in both CLMcrop and LPJ-GUESS (Figure 16). The same is true for rice, where parts of Africa and Asia go from having positive impacts to future rice yields under climate change, to negative when protein is accounted for (Figure 16). CLMcrop and LPJ-GUESS both show very similar regional impacts to both yield and protein yield under future climate change. Figure 17 shows regional impacts to yield and protein yield under future SAI

relative to future climate change. Again, incorporating impacts to protein causes future yield changes under SAI to go from being positive to negative in some places. In CLMcrop, impacts to wheat go from being positive under SAI to negative in parts of Africa, Eastern Europe, and Southeast Asia (Figure 17). Rice yields become negative in CLMcrop in parts of South America and India, and maize impacts under SAI become negative in CLMcrop in many parts of Africa and South America when looking at protein yield (Figure 17). Figure 18 shows the regional impacts under SAI of looking at protein yield relative to just yield. Figure 18 makes it clearer where impacts under SAI change when switching from looking at yield to protein yield. There are small decreases to impacts of wheat in parts of Eastern Europe in LPJ-GUESS, and decreases to rice yields in parts of Africa, South America, and Southeast Asia in LPJ-GUESS (Figure 18). pDSSAT shows large decreases to maize in almost all areas where maize is grown when looking at protein yield instead of yield (Figure 18). Since CO₂ concentrations are the same under ARISE-SAI and SSP2-4.5, these impacts to yield and protein are driven mainly by temperature. Some areas may have increases to yield under SAI from reduced heat stress, accompanied by decreases to protein due to higher carbon content without an equal increase in Nitrogen uptake. These impacts to yield and protein from reduced temperatures under SAI act to oppose each other. It seems model dependent how large of an impact changes to protein will have on protein yields. pDSSAT shows large decreases to maize when accounting for protein, while CLMcrop shows only moderate decreases in some areas, and LPJ-GUESS shows small impacts from including protein (Figure 18). While impacts to global crop yields tend to be made worse under SAI when accounting for protein, the impacts relative to climate change are still generally positive for most crops and models (Figure 17). Using more crop and climate models and continuing to account for crop protein changes is important to understand the full picture of how SAI may affect global agriculture.

Section 4.0: Discussion

Section 4.1: Optimal climate intervention scenarios for crop production vary by nation

Using a state-of-the-art climate model coupled to a crop model, impacts on crop production under 11 future climate change and climate intervention scenarios were analyzed (Table 1). Then, offline crop model simulations were run to better understand what changes to the climate are contributing to the impacts of SAI on maize, rice, soybean and spring wheat production.

CESM2(WACCM6) showed a satisfactory ability to model crops and their interaction with the Earth system and was included in Coupled Model Intercomparison Project Phase 6 (CMIP6) (Danabasoglu et al., 2020). CLM5crop has also been tested substantially (Fan et al., 2021; Lombardozzi et al., 2020; Lawrence et al., 2019; Fisher et al., 2019). CLM5crop did a reasonable job capturing interannual variability in global and national yields from a historic period (Supplementary Figure 12). The CLM5crop historical simulation portrayed in Supplementary Figure 22 was run at 2° resolution using the GSWP3 atmospheric forcing data with transient climate, CO₂, nitrogen deposition, land-cover change, irrigation and fertilization (Dirmeyer et al., 2006). The yield time series in Supplementary Figure 12 were detrended since differences in the magnitude and trend of yield are primarily due to cultivars, technology, planting and harvest dates, irrigation and fertilization practices in the real world that are not relevant to this study. A non-detrended version of Supplementary Figure 12 was also included to better compare to other studies (Supplementary Figure 13). The interannual variability of national yield reported by the Food and Agriculture Organization Corporate Statistical Database (FAOSTAT) is the combined result of changing agriculture management and interannual climate variation. In the model simulation, the interannual variability of yield is mainly due to climate variability. CLM5crop shows larger rice yield variation than FAOSTAT for some countries, which is a known issue of seasonality within

CLM5crop for Southeast Asia that is currently being updated (Rabin et al., 2023). Also, FAOSTAT reports yields for a certain year according to when most of the growing season for a nation occurs, so the time series of simulated historical yields in Supplementary Figure 12 was shifted by one year if the correlation coefficient with the FAOSTAT time series was increased by at least 0.3 to better compare similarities in interannual variability (FAO, 2022; Müller et a., 2017). CLM5crop's ability to simulate national time series of crop yield and production is comparable to that of other state-of-the-art process-based crop models (Müller et a., 2017). While no crop model is perfect, CLM5crop's interannual response to changing climate makes it a valuable tool to understand how national yield and production will change under future climate scenarios. CLM5crop still needs to be improved with a better representation of impacts from extreme weather events, the inclusion of ultraviolet radiation impacts on crops and surface ozone impacts on crops, and updated assumptions about changing future agricultural planting and harvesting dates. Uncertainties in future changes to nitrogen fertilization and how CLM5crop handles CO₂ fertilization and responses to climate (such as temperature change) are areas of ongoing work. CLM5crop currently plants spring wheat everywhere wheat is grown. Including winter wheat in the future could impact the results. Moreover, to ensure a robust understanding of crop responses to different climate scenarios, a multi-crop model assessment is needed, since the findings of this study are derived from only a single model, and the inclusion of other models could lead to variations in the results. Further work is needed to update the model to include these parameters to paint a more complete picture of potential impacts on crops due to SAI, and analysis using multiple climate and crop models is needed to help reduce uncertainties.

Section 4.2: Maize yield changes under sulfate aerosol climate intervention using three global gridded crop models

Despite the detailed process representation of these models, highly diverse results are still observed. CESM2(WACCM6) showed a satisfactory ability to simulate past climate and was included in the Coupled Model Intercomparison Project Phase 6 (CMIP6) (Danabasoglu et al., 2020). All three crop models have been tested substantially. pDSSAT contributed to the Global Gridded Crop Model Intercomparison (GGCMI) Project Phase 3 simulations, which assessed impacts to global crop production under future climate change (Jägermeyr et al., 2021). LPJ-GUESS contributed to the GGCMI phase 2 simulations (Franke et al., 2020). All three crop models were evaluated together to test for their ability to simulate global and regional interannual yield variability in the GGCMI phase 1 evaluation (Müller et al., 2017). CLM5crop's ability to simulate past interannual changes to global and regional crop production has been tested in several other studies (Lombardozzi et al., 2020; Fan et al., 2021; Clark et al., 2023).

While this study uses three crop models, it is limited by only using one ensemble member from one climate model and one SAI scenario. Using additional ensemble members in the future would provide more robust results by limiting noise due to natural climate variability. CESM2 is warm relative to observations, so using other climate models could help to reduce climate model uncertainty (Danabasoglu et al., 2020). Using bias correction in the future could also help to reduce any uncertainties introduced by the climate model but was not done in this study. While using three global crop models is an improvement upon past SAI impact studies, rigor would be increased by including additional models that feature the required process representations. Global gridded crop models show very large uncertainty of production impacts under future climate change, and crop model uncertainty is much larger than uncertainty stemming from climate models (Jägermeyr et

al., 2021). This study serves as a first step for a more robust analysis of crop impacts from SAI, and more crop models are needed to simulate SAI impacts. It would also be beneficial to incorporate other impact models, such as fisheries models, to understand how food production will change both on land and in the ocean under SAI.

SAI would impact ultraviolet (UV) radiation and surface ozone, which are both important driving factors for crop production (NASEM, 2021). This study did not include the impacts on maize from changing UV radiation and surface ozone. While including surface ozone impacts in global process-based crop models is a new area of model improvement, no global process-based crop model currently has the capability to simulate impacts from changing UV radiation. Improving the crop models and incorporating these impacts in future SAI crop modeling studies will be important to understanding the full story of how SAI would impact global crop production.

Section 4.3 Stratospheric sulfate aerosol climate intervention could reduce the nutritional value of maize and rice

This study serves as a first step assessment of potential impacts to global crop protein changes under both future climate change and climate intervention using multiple global gridded crop models. The three crop models used here show varying response to crop yield and protein under future climate change and SAI. The ability of CLMcrop, LPJ-GUESS, and pDSSAT to simulate historical crop yields has been validated in previous studies. pDSSAT was able to replicate the interannual variability of historical maize yields with a correlation coefficient of 0.88 (Müller et al., 2017). LPJ-GUESS replicated the interannual variability of historical yields of wheat, rice, soybean, and maize with correlation coefficients of 0.60, 0.52, -0.00, and 0.71, respectively (Müller et al., 2017). The same analysis was done for CLMcrop, where it replicated the interannual variability of historical yields of wheat, rice, soybean, and maize with correlation coefficients of 0.52, 0.40, 0.23, and 0.91, respectively (Clark et al., 2023). There is no global

dataset for observations of crop protein, so a similar analysis cannot be done for protein. However, CLMcrop did a reasonable job capturing changes to protein under elevated CO₂ when compared to observations from FACE experiments (Supplementary Figure 1; Myers et al., 2014). There is a lack of laboratory and field experiments that test how crop protein responds to elevated temperature, and more data on crop responses to current climate are needed for better model validation.

Process-based crop models like CLM5crop, LPJ-GUESS, and pDSSAT simulate key processes of the Nitrogen cycle, including Nitrogen fixation, plant Nitrogen uptake from the soil, atmospheric Nitrogen deposition, leaching, nitrification and denitrification. CLM5crop and LPJ-GUESS are full ecosystem models and include additional processes like Nitrogen losses due to fire that are not included in pDSSAT. More general ecosystem models like CLM5crop and LPJ-GUESS lack representation of certain processes important for the Nitrogen cycle, such as nutrient competition between plant types, soil microbial communities, heterogenous soil layers, and long-term Nitrogen accumulation in soil. There are also differences between the three models used here. While CLM5crop and LPJ-GUESS are both ecosystem models, they differ in how they represent plant nitrogen uptake. CLM5crop calculates plant nitrogen uptake using the Fixation and Uptake of Nitrogen (FUN) model (Lawrence et al., 2019). In the FUN model a plant can expend energy in the form of carbon to uptake nitrogen from several possible sources. LPJ-GUESS determines Nitrogen demand and uptake to maintain optimal leaf Nitrogen for photosynthesis (Smith et al., 2014). Since pDSSAT is developed as a site-based agriculture model instead of an ecosystem model, it includes some processes important to the nitrogen cycle that CLM5crop and LPJ-GUESS do not, such as mineralization and immobilization (Jones et al., 2003). Differences between model

representation of nitrogen cycle processes could explain some differences in results how future responses to crop protein concentrations.

This study is limited by using only one ensemble member from one climate model, one SAI scenario, and only three crop models. A more comprehensive analysis using climate forcings from multiple scenarios and climate models with additional global gridded crop models is needed to draw more robust conclusions and reduce uncertainties. Current crop models are not able to simulate impacts from changing surface ozone and ultraviolet radiation, which are both expected to be modified under SAI (NASEM, 2021). Updating the models to handle these climate changes under SAI is needed to better understand the full impacts of SAI on crop yield and protein. While these models can estimate protein concentrations through simulated grain C:N ratios, they do not have the ability to simulate other important nutrients, such as Iron and Zinc, which have been shown to also be impacted by CO₂ and temperature changes (Köhler et al., 2019). While these simulations applied constant fertilizer application, applying additional fertilizer may be able to mitigate negative impacts on crop protein concentrations, but would be accompanied by negative environmental effects, such as air pollution, stratospheric ozone depletion, and eutrophication (Yin et al., 2021).

Section 5.0: Conclusions

Limiting global warming from anthropogenic greenhouse gas forcing using SAI benefits global production of maize, rice, soybean and wheat relative to climate change without SAI under all the scenarios analyzed in CLM5crop. Climate intervention to limit anthropogenic warming while maintaining elevated CO₂ increases global calories from maize, rice, soybean and wheat by 12–24% during the decade 2060–2069, depending on the scenario, which is consistent with the most recent SAI crop modelling study that also used CLM5crop but a different climate model (Fan et al., 2021). Benefits to crop production from SAI relative to climate change without SAI are dominated by heat-stress reduction. Solar dimming to represent SAI impacts on crops underestimates yields due to lacking a representation of diffuse radiation fertilization. Diffuse fertilization may dominate the yield response to radiative changes under small amounts of SAI, but larger amounts of aerosols may decrease yields due to a reduction in total solar radiation (Proctor et al., 2021). Although global production increases under SAI, there are production decreases for top producers of each crop under all climate intervention scenarios. It cannot be easily argued that trade can offset regional losses under SAI, as the world currently produces enough food to feed everyone on the planet, yet many still face food insecurity and starvation due to crop production being unevenly distributed around the world (Rabin et al., 2023). These patterns of regional food insecurity could be shifted or exacerbated by SAI implementation, making regional crop impacts from SAI an important consideration. High-latitude regions such as Russia and Canada show the largest decreases in crop production under climate intervention relative to climate change. The number of countries that produce fewer calories under SAI relative to climate change increases with more temperature limitation. No SAI temperature target benefits everyone. Different parts of the world maximize calories from crops under different temperature targets, with

higher-latitude nations producing the most calories under unabated global warming, midlatitude nations under moderate temperature limitation and equatorial nations maximizing calories under high levels of climate intervention.

These results introduce important governance concerns related to SAI deployment. Although crop production in most nations increases under SAI relative to climate change, there would probably be decreases relative to warming in several top producing nations. Nations that do increase crop production under SAI would prefer different temperature targets to maximize the calories produced from crops. How would SAI deployment be governed? Many have argued that since SAI would impact all nations, universal agreement on deployment would be needed (Reynolds et al., 2019). If an international group was charged with making a decision that accounted for the will of all or most nations in the world, coming to a decisive agreement would be challenging. It has also been argued that nations that would be harmed by SAI could be compensated in some way (Reynolds et al., 2019). This method is unproven and would be challenging for many reasons. Associating climate or extreme weather impacts with SAI rather than with natural variability would be difficult (Reynolds et al., 2019; Svoboda et al., 2014). Would harmful impacts be compared with some historical climate, or with the future climate without SAI (Reynolds et al., 2019; Bunzl et al., 2019)? Crop production is only a single metric, and incorporating the responses of other impact metrics to varying levels of climate intervention would only complicate the issue. Further work to better quantify the impacts of SAI and how SAI could be effectively governed is still needed to aid policymakers in decision making.

Crop models introduce large uncertainties when simulating agricultural responses to future climate changes. Placing sulfate aerosols in the stratosphere to maintain surface temperatures of 1.5°C above preindustrial levels caused maize production to increase by 0% in LPJ-GUESS, 4%

in CLMcrop and 11% in pDSSAT over the years 2049-2068 under SSP2-4.5-SAI-1.5C relative to SSP2-4.5. CLM5crop and pDSSAT show benefits due to reduced heat stress under SAI, while LPJ-GUESS had a lower sensitivity to temperature, causing impacts under SAI and climate change to be globally very similar. CLM5crop and pDSSAT are less sensitive to other climate variables, like precipitation, and therefore the temperature impact dominated the overall response (Clark et al., 2023; Müller et al., 2024). CLMcrop and pDSSAT showed almost no areas of significant reduction of maize yield under SAI relative to climate change, and LPJ-GUESS showed no significant changes to maize yield anywhere in the world under SAI. pDSSAT had a large benefit to future maize production under SAI relative to climate change, CLM5crop had a moderate benefit, and LPJ-GUESS shows almost no difference between SAI and climate change. This model-dependent response to maize yield under SAI highlights remaining uncertainty in the global temperature response of maize production under both future climate change and possible SAI implementation. In the scenario and models used, enhanced diffuse fertilization has a very small impact on global maize production. Using multiple climate models which can produce diffuse radiation output and multiple crop models which can simulate diffuse radiation fertilization effects could help to further constrain remaining uncertainties in the process-based crop model response to changing radiation under SAI. Improving model development and utilizing additional crop models, climate models, and SAI scenarios will be necessary to better understand possible impacts to maize production and inform future policy decisions, and there is no clear answer yet as to how global maize may be impacted by SAI.

In addition, climate change and SAI would not only affect agriculture production, but also influence food quality. Stratospheric aerosol climate intervention used to maintain 1.5°C above preindustrial levels relative to SSP2-4.5 causes global maize protein to change by -3.8%, 0.9%,

and -2.3% for CLMcrop, LPJ-GUESS, and pDSSAT, respectively. Wheat protein changes by -1.4% and -0.1%, global rice protein changes by -4.1% and -0.9%, and soybean protein changes by 0.2% and 0.6% in CLMcrop and LPJ-GUESS. While global crop yields tend to increase under SAI relative to climate change, accounting for these changes to protein causes crop yields benefits to change by -4.1%, 1.0%, and -2.5% for maize in CLMcrop, LPJ-GUESS, and pDSSAT. Wheat yield benefits under SAI are changed by 0.5% and -0.2%, rice yields by -3.7% and -1.4% and soybean yields change by 0.3% and 0.0% in CLMcrop and LPJ-GUESS. Despite CO₂ concentrations being the same in the SAI and climate change scenarios, reducing temperature increases with SAI has the potential to reduce protein and protein yields of maize and rice, while wheat and soybean are minimally impacted by protein changes under SAI. Overall benefits to protein yield are still mostly positive for all four crops under SAI relative to climate change. Additional work is needed to run more SAI scenarios with more climate and crop models. Accounting for changes to protein as well as yields will be important for understanding the full impact of SAI on future global agriculture productivity.

Section 6.0: Data and code availability

Section 6.1: Optimal climate intervention scenarios for crop production vary by nation

Output from the CESM2(WACCM6) SSP2-4.5 and SSP2-4.5-1.5 °C is freely available at <https://doi.org/10.26024/0cs0-ev98>. CESM2(WACCM6) output from SSP5-8.5, SSP5-3.4-OS, Geoengineering Model Intercom-parison Project G6Solar and G6Sulfur is freely available on Earth System Grid at <https://esgf-node.llnl.gov/search/cmip6/>. CESM2(WACCM6) output from SSP5-3.4-OS-2.0 °C, SSP5-3.4-OS-1.5 °C and SSP5-8.5-1.5 °C is available at <https://doi.org/10.26024/t49k-1016>. Coupled and offline CLM5crop postprocessed yield data are available at <https://doi.org/10.6084/m9.figshare.24085797.v1>. Historical yield observation data were obtained from FAOSTAT at <https://www.fao.org/faostat/en/#data>. The source code for the CESM(WACCM) model used in this study is freely available at https://www.cesm.ucar.edu/working_groups/Whole-Atmosphere/code-release.html, and the code for CLM5 is available at <https://www.cesm.ucar.edu/models/cesm2/land/>. Postprocessing and figure generation scripts can be found at https://github.com/bjc204/Clark_etal_NatureFood_2023.

Section 6.2: Maize yield changes under sulfate aerosol climate intervention using three global gridded crop models

Climate model output is available at <https://doi.org/10.26024/0cs0-ev98>. Crop model output is available at <https://doi.org/10.6084/m9.figshare.25944274.v1>. Figure generation code is available at https://github.com/bjc204/Clarketal_EarthsFuture_24.git. The source code for the CESM(WACCM) model used in this study is freely available at https://www.cesm.ucar.edu/working_groups/Whole-Atmosphere/code-release.html. The code for CLM5 is available at <https://www.cesm.ucar.edu/models/cesm2/land/>. The code for LPJ-GUESS

is available at <https://web.nateko.lu.se/lpj-guess/download.html>. The code for DSSAT is available at <https://dssat.net/source-code/>.

Section 6.3 Stratospheric sulfate aerosol climate intervention could reduce the nutritional value of maize and rice

Climate model output is available at <https://doi.org/10.26024/0cs0-ev98>. Crop model output is available at <https://doi.org/10.6084/m9.figshare.25944274.v1>. Figure generation code is available at <https://github.com/bjc204.git>.

Section 7.0: References

- Ainsworth, E. A., Rogers, A. The response of photosynthesis and stomatal conductance to rising [CO₂]: mechanisms and environmental interactions. *Plant Cell Environ.*, **30**, 258–270 (2010). doi:10.1111/j.1365-3040.2007.01641.x
- Ainsworth E., Long S. 30 years of free-air carbon dioxide enrichment (FACE): What have we learned about future crop productivity and its potential for adaptation? *Glob Change Biol.*, **27**, 27–49 (2020). doi.org/10.1111/gcb.15375
- Bala, G., Duffy, P. B., and Taylor, K. E. Impact of geoengineering schemes on the global hydrological cycle, *Proc. Nat. Acad. Sci.*, **105**, 7664–7669 (2008). doi:10.1073/pnas.0711648105
- Bloom, A. J. et al. Carbon Dioxide Enrichment Inhibits Nitrate Assimilation in Wheat and Arabidopsis. *Science*, **328**, 899–903 (2010). doi:10.1126/science.1186440
- Bunzl, M. Geoengineering harms and compensation. *Stanf. J. Law Sci. Policy*, **4**, 69–75 (2019).
- Chunwu, Z. et al. Carbon dioxide (CO₂) levels this century will alter the protein, micronutrients, and vitamin content of rice grains with potential health consequences for the poorest rice-dependent countries. *Sci. Adv.*, **4** (2018). doi:10.1126/sciadv.aaq1012
- Clark, B. et al. Optimal climate intervention scenarios for crop production vary by nation. *Nat. Food*, **4**, 902–911 (2023). doi.org/10.1038/s43016-023-00853-3
- Collatz, G. J., Ribas-Carbo, M., and Berry, J. A. Coupled photosynthesis-stomatal conductance model for leaves of C4 plants, *Funct. Plant Biol.*, **19**, 519–538 (1980). doi:10.1093/aob/mcg080
- Cotrufo, MF, Ineson, P, Scott, A. Elevated CO₂ reduces the nitrogen concentration of plant tissues. *Global Change Biology*, **4**, 43–54 (1998).
- Crutzen, P., J. Albedo enhancement by stratospheric sulfur injections: A contribution to resolve a policy dilemma?, *Climate Change*, **77**, 211–219 (2006). doi:10.1007/s10584-006-9101-y
- Danabasoglu, G., Lamarque, J.-F., Bacmeister, J., Bailey, D. A., DuVivier, A. K., Edwards, J., et al. The Community Earth System Model Version 2 (CESM2). *Journal of Advances in Modeling Earth Systems*, **12**, e2019MS001916 (2020). <https://doi.org/10.1029/2019MS001916>
- Davis, N. A., Visioni, D., Garcia, R. R., Kinnison, D. E., Marsh, D. R., Mills, M., et al. Climate, variability, and climate sensitivity of “Middle Atmosphere” chemistry configurations of the Community Earth System Model Version 2, Whole Atmosphere Community Climate Model Version 6 (CESM2(WACCM6)). *Journal of Advances in Modeling Earth Systems*, **15** (2023). doi.org/10.1029/2022MS003579
- Dirmeyer, P. A. et al. GSWP-2, multimodel analysis and implications for our perception of the land surface. *Bull. Am. Meteorol. Soc.* **87**, 1381–1398 (2006).
- Eastham, S., Keith, D., and Barrett, S. Mortality tradeoff between air quality and skin cancer from changes in stratospheric ozone, *Environ. Res. Lett.*, **13** (2018). doi:10.1088/1748-9326/aaad2e
- Elliott, J. et al. The parallel system for integrating impact models and sectors (pSIMS). *Environmental Modelling & Software*, **62**, 509–516. (2014). <https://doi.org/10.1016/j.envsoft.2014.04.008>
- Fan, Y., Tjiputra, J., Muri, H., Lombardozzi, D., Park, E. U., Wu, S., Keith, D. Solar geoengineering can alleviate climate change pressures on crop yields. *Nature Food*, **2**, 373–381 (2021). doi:10.1038/s43016-021-00278-w

- FAO (Food and Agricultural Organization): Food Balance Spreadsheets,
<https://www.fao.org/faostat/en/#data/FBS>, accessed 20 July 2022.
- Farquhar, G., Caemmerer, S., and Berry, J. A biochemical model of photosynthetic CO₂ assimilation in leaves of C3 species. *Planta*, **149**, 78–90 (1992). doi:10.1007/BF00386231
- Fernando, N. et al. Rising atmospheric CO₂ concentration affects mineral nutrient and protein concentration of wheat grain. *Food Chemistry*, **133**, 1307–1311 (2012). doi:10.1016/j.foodchem.2012.01.105
- Fisher, R. A., Wieder, W. R., Sanderson, B., Koven, C. D., Oleson, K. W., Xu, C., et al. Parametric controls on vegetation responses to biogeochemical forcing in the CLM5. *Journal of Advances in Modeling Earth Systems*, **11**, 2879–2895 (2019). doi:10.1029/2019MS001609
- Franke, J. et al. The GGCMI Phase 2 experiment: global gridded crop model simulations under uniform changes in CO₂, temperature, water, and nitrogen levels (protocol version 1.0). *Geosci. Model Dev.*, **13**, 2315–2336 (2020). <https://doi.org/10.5194/gmd-13-2315-2020>
- Fugile, P. Climate change upsets agriculture, *Nature Climate Change*, **11**, 293–299 (2021). doi:10.1038/s41558-021-01017-6
- Greenwald, R. et al. The influence of aerosols on crop production: A study using the CERES crop model. *Agricultural Systems*, **89** (2006). doi.org/10.1016/j.aghsy.2005.10.004
- Gifford, RM, Barrett, D.J, Lutze, J.L. The effects of elevated [CO₂] on the C:N and C:P mass ratios of plant tissues. *Plant and Soil*, **224**, 1–14 (2000).
- Gu, L. et al. Response of a deciduous forest to the Mount Pinatubo eruption: enhanced photosynthesis. *Science*, **299**, 2035–2038 (2003). 10.1126/science.1078366
- Guo, X. et al. T-FACE studies reveal that increased temperature exerts an effect opposite to that of elevated CO₂ on nutrient concentration and bioavailability in rice and wheat grains. *Food Energy Secur.* **11**, 1–19 (2022).
- Heckendorf, P., Weisenstein, D., Fueglister, S., Luo, B. P., Rozanov, E., Schraner, M., Thomason, L. W., and Peter, T. 2009: The impact of geoengineering aerosols on stratospheric temperature and ozone, *Environ. Res. Lett.*, **4**, 045108 (2009). doi:10.1088/1748-9326/4/4/045108
- Henry, M., et al. Comparison of UKESM1 and CESM2 simulations using the same multi-target stratospheric aerosol injection strategy, *Atmos. Chem. Phys.*, **23**, 13369–13385 (2023). doi.org/10.5194/acp-23-13369-2023
- Hoogenboom, G., Porter, C. H., Boote, K. J., Shelia, V., Wilkens, P. W., Singh, U., White, J. W., Asseng, S., Lizaso, J. I., Moreno, L. P., Pavan, W., Ogoshi, R., Hunt, L. A., Tsuji, G. Y., and Jones, J. W. The DSSAT crop modeling ecosystem, in: Advances in Crop Modeling for a Sustainable Agriculture, edited by: Boote, K. J., Burleigh Dodds Science Publishing, Cambridge, United Kingdom, 173–216, (2019). doi.org/10.19103/AS.2019.0061.10
- Jägermeyr, J., Müller, C., Ruane, A.C. et al. Climate impacts on global agriculture emerge earlier in new generation of climate and crop models. *Nat. Food*, **2**, 873–885 (2021) doi:10.1038/s43016-021-00400-y.
- Jones, C.A., and J.R. Kiniry (Eds.). CERES-Maize: A simulation model of maize growth and development. Texas A&M Univ. Press, College Station. (1986)
- Jones, A., Haywood, J. M., Alterskjær, K., Boucher, O., Cole, J. N. S., Curry, C. L., Irvine, P. J., Ji, D., Kravitz, B., Kristjánsson, J. E., Moore, J. C., Niemeier, U., Robock, A., Schmidt, H., Singh, B., Tilmes, S., Watanabe, S., and Yoon, J-H. The impact of abrupt suspension of solar radiation management (termination effect) in experiment G2 of the Geoengineering Model

- Intercomparison Project (GeoMIP), *J. Geophys. Res.-Atmos.*, **118**, 9743–9752 (2013). doi:10.1002/jgrd.50762
- Köhler, I. H., Huber, S. C., Bernacchi, C. J. & Baxter, I. R. Increased temperatures may safeguard the nutritional quality of crops under future elevated CO₂ concentrations. *Plant J.* **97**, 872–886 (2019).
- Kravitz, B., Robock, A., Tilmes, S., et al. The Geoengineering Model Intercomparison Project Phase 6 (GeoMIP6): simulation design and preliminary results, *Geosci. Model Dev.*, **8**, 3379–3392 (2015). doi:10.5194/gmd-8-3379-2015, 2015.
- Kravitz, B., MacMartin, D. G., Mills, M. J., Richter, J. H., Tilmes, S., Lamarque, J.-F., Vitt, F. First simulations of designing stratospheric sulfate aerosol geoengineering to meet multiple simultaneous climate objectives. *Journal of Geophysical Research: Atmospheres*, **122**, 12,616–12,634 (2017). doi:10.1002/2017JD026874
- Kummu, M., Heino, M., Taka, M., Varis, O., Viviroli, D. Climate change risks pushing one-third of global food production outside the safe climatic space. *One Earth*, **4**, 720–729 (2021). doi:10.1016/j.oneear.2021.04.017
- Lawrence, D. M., Fisher, R. A., Koven, C. D., Oleson, K. W., Swenson, S. C., Bonan, G., et al. The Community Land Model version 5: Description of new features, benchmarking, and impact of forcing uncertainty. *J. Adv. Modeling Earth Sys.*, **11**, 4245–4287 (2019). doi:10.1029/2018MS001583
- Lindeskog, M. et al. Implications of accounting for land use in simulations of carbon cycling in Africa. *Earth System Dynamics*, **4**, 385–407 (2013). doi.org/10.5194/esd-4-385-2013
- Lombardozzi, D. L., et al. Simulating agriculture in the Community Land Model Version 5. *Journal of Geophysical Research: Biogeosciences*, **125**, e2019JG005529 (2020). doi:10.1029/2019JG005529
- MacMartin, D., Visioni, D., Kravitz, B., et al. Scenarios for modeling solar radiation modification, *Proc. Nat. Acad. Sci.*, **119** (2022). doi:10.1073/pnas.2202230119
- Mbow, C. et al. *Special Report on Climate Change and Land* (eds Shukla, P. R. et al.) 437–550 (IPCC) (2019). <https://www.ipcc.ch/site/assets/uploads/2019/11/SRCCCL-Full-Report-Compiled-191128.pdf>
- Meinshausen, M., Nicholls, Z. R. J., Lewis, J., Gidden, M. J., Vogel, E., Freund, M., et al. The shared socio-economic pathway (SSP) greenhouse gas concentrations and their extensions to 2500. *Geoscientific Model Development*, **13**, 3571–3605 (2020). doi.org/10.5194/gmd-13-3571-2020
- Müller, C. et al. Global gridded crop model evaluation: benchmarking, skills, deficiencies and implications. *Geosci. Model Dev.*, **10**, 1403–1422 (2017). doi.org/10.5194/gmd-10-1403-2017
- Müller, C., Jägermeyr, J., Franke, J. A., Ruane, A. C., Balkovic, J., Ciais, P., et al. Substantial differences in crop yield sensitivities between models call for functionality-based model evaluation. *Earth's Future*, **12**, e2023EF003773 (2024). doi.org/10.1029/2023EF003773
- Myers, S., Zanobetti, A., Kloog, I. et al. Increasing CO₂ threatens human nutrition. *Nature*, **510**, 139–142 (2014). doi.org/10.1038/nature13179
- National Academies of Sciences, Engineering, and Medicine [NASEM]. Reflecting Sunlight: Recommendations for Solar Geoengineering Research and Research Governance. *National Academies Press* (2021). doi.org/10.17226/25762
- O’Neil, B. C., et al. The Scenario Model Intercomparison Project (ScenarioMIP) for CMIP6, *Geosci. Model Dev.*, **9**, 3461–3482 (2016). doi:10.5194/gmd-9-3461-2016

- Pitari, G., Aquila, V., Kravitz, B., Robock, A., Watanabe, S., Cionni, I., De Luca, N., Di Genova, G., Mancini, E., and Tilmes, S. Stratospheric ozone response to sulfate geoengineering: Results from the Geoengineering Model Intercomparison Project (GeoMIP), *J. Geophys. Res.-Atmos.*, **119**, 2629–2653 (2014). doi:10.1002/2013JD020566
- Pongratz, J., Lobell, D. B., Cao, L., and Caldeira, K. Crop yields in a geoengineered climate, *Nature Clim. Change*, **2**, 101–105 (2012). doi:10.1038/nclimate1373
- Portmann, F. T., Siebert, S. & Döll, P. MIRCA2000—Global monthly irrigated and rainfed crop areas around the year 2000: a new high-resolution data set for agricultural and hydrological modeling. *Global Biogeochem. Cycles*, **24** (2010). doi.org/10.1029/2008GB003435
- Proctor, J., et al. Estimating global agricultural effects of geoengineering using volcanic eruptions, *Nature*, **560**, 480–483 (2018). doi:10.1038/s41586-018-0417-3
- Rabin, S. S., Sacks, W. J., Lombardozzi, D. L., Xia, L. & Robock, A. Observation-based sowing dates and cultivars significantly affect yield and irrigation for some crops in the Community Land Model (CLM5). *Geoscientific Model Development*, **16**, 7253–7273 (2023). doi.org/10.5194/gmd-2023-66
- Rasch, P. J., Crutzen, P. J., and Coleman, D. B. Exploring the geoengineering of climate using stratospheric sulfate aerosols: the role of particle size, *Geophys. Res. Lett.*, **35**, L02809 (2008). doi:10.1029/2007GL032179
- Reynolds, J. L. Solar geoengineering to reduce climate change: a review of governance proposals. *Proc. R. Soc. A*, (2019). doi.org/10.1098/rspa.2019.0255
- Richter, J. H., Visioni, D., MacMartin, D. G., Bailey, D. A., Rosenbloom, N., Dobbins, B., Lee, W. R., Tye, M., and Lamarque, J.-F. Assessing Responses and Impacts of Solar climate intervention on the Earth system with stratospheric aerosol injection (ARISE-SAI): protocol and initial results from the first simulations, *Geosci. Model Dev.*, **15**, 8221–8243 (2022). doi.org/10.5194/gmd-15-8221-2022
- Robock, A. 20 reasons why geoengineering may be a bad idea, *Bull. Atomic Sci.*, **64**, 14–18 (2008). doi:10.2968/064002006
- Roderick, M. L., Farquhar, G. D., Berry, S. L. & Noble, I. R. On the direct effect of clouds and atmospheric particles on the production and structure of vegetation. *Oecologia* **129**, 21–30 (2001). doi.org/10.1007/s004420100760
- Rosenzweig, C., et al. Assessing agricultural risks of climate change in the 21st century in a global gridded crop model intercomparison, *Proc. Nat. Acad. Sci.*, **111**, 3268–3273 (2014). doi:10.1073/pnas.1222463110
- Schiferl, L. D., Heald C. L. & Kelly, D. Resource and physiological constraints on global crop production enhancements from atmospheric particulate matter and nitrogen deposition. *Biogeosciences*, **15**, 4301–4315 (2018). doi.org/10.5194/bg-15-4301-2018
- Shukla, P. R. et al. Special Report on Climate Change and Land, *IPCC 2019*, 437–550 (2019). doi.org/10.1017/9781009157988
- Smith, B. et al. Implications of incorporating N cycling and N limitations on primary production in an individual-based dynamic vegetation model. *Biogeosciences*, **11**, 2027–2054 (2014). doi.org/10.5194/bg-11-2027-2014
- Svoboda, T. & Irvine, P. Ethical and technical challenges in compensating for harm due to solar radiation management geoengineering. *Ethics Policy Environ.* **17**, 157–174 (2014).
- Taub, D. et al. Effects of elevated CO₂ on the protein concentration of food crops: a meta-analysis. *Global Change Biology*, **14**, 565–575. (2008). doi:10.1111/j.1365-2486.2007.01511.x

- Tilmes, S., Müller, R., and Salawitch, R.: The sensitivity of polar ozone depletion to proposed geoengineering schemes, *Science*, **320**, 1201–1204 (2008). doi:10.1126/science.1153966
- Tilmes, S., et al. Reaching 1.5 and 2.0°C global surface temperature targets using stratospheric aerosol geoengineering, *Earth Syst. Dynam.*, **11**, 579–601 (2020). doi:10.5194/esd-11-579-2020
- Visioni, D., MacMartin, D., Kravitz, B., et al. Identifying the sources of uncertainty in climate model simulations of solar radiation modification with the G6sulfur and G6solar Geoengineering Model Intercomparison Project (GeoMIP) simulations, *Atmos. Chem. Phys.*, **21**, 10039–10063 (2021). doi:10.5194/acp-21-10039-2021
- Wang, J., Hasegawa, T., Li, L., Lam, S.K., Zhang, X., Liu, X. and Pan, G. Changes in grain protein and amino acids composition of wheat and rice under short-term increased [CO₂] and temperature of canopy air in a paddy from East China. *New Phytol*, **222**: 726-734 (2019). doi.org/10.1111/nph.15661
- Wigley, T. M. A Combined Mitigation/Geoengineering Approach to Climate Stabilization, *Science*, **314**, 452-454 (2006). doi:10.1126/science.1131728
- Xia, L., Nowack, P. J., Robock, A., and Tilmes, S. Impacts of stratospheric sulfate geoengineering on tropospheric ozone. *Atmos. Chem. Phys.*, **17**, 11,913-11,928 (2017). doi:10.5194/acp-17-11913-2017
- Xia, L., Robock, A., Cole, J., Curry, C. L., Ji, D., Jones, A., Kravitz, B., Moore, J. C., Muri, H., Niemeier, U., Singh, B., Tilmes, S., Watanabe, S., and Yoon, J.-H. Solar radiation management impacts on agriculture in China: A case study in the Geoengineering Model Intercomparison Project (GeoMIP), *J. Geophys. Res.-Atmos.*, **119**, 8695–8711 (2014). doi:10.1002/2013JD020630.
- Yang, H., et al. Potential negative consequences of geoengineering on crop production: A study of Indian groundnut. *Geophys. Res. Lett.*, **43**, 11,786-11,795 (2016). doi:10.1002/2016GL071209
- Yin, Y. et al. Climate change increases Nitrogen concentration in rice with low Nitrogen use efficiency. *Earth's Future*, **9** (2021). doi.org/10.1029/2020EF001878
- Zhan, P., et al. Impacts of sulfate geoengineering on rice yield in China: Results from a multimodel ensemble, *Earth's Future*, **7**, 395-410 (2019). doi:10.1029/2018EF001094.
- Zhao, M., Cao, L., Visoni, D., & MacMartin, D. G. Carbon cycle response to stratospheric aerosol injection with multiple temperature stabilization targets and strategies. *Earth's Future*, **12** (2024). doi.org/10.1029/ 2024EF004474

Section 8.0: Table and Figures

Table 1. Scenario names for climate change and climate intervention simulations with years of the simulations, and number of ensemble members.

Scenario	Years of Analyses	Ensemble Members	Mean Temperature over Cropland (°C) (2060-2069)
SSP2-4.5	2015-2070	10	19.6
SSP2-4.5-1.5°C	2035-2070	10	18.6
SSP2-4.5-1.0°C	2035-2070	2	17.6
SSP2-4.5-0.5°C	2035-2070	2	17.0
SSP5-3.4-OS	2040-2100	3	20.1
SSP5-3.4-2.0°C	2040-2100	3	19.0
SSP5-3.4-1.5°C	2040-2100	3	18.3
SSP5-8.5	2020-2100	3	21.0
SSP5-8.5-1.5°C	2020-2100	3	18.4
G6Solar [SSP5-8.5]	2020-2100	2	19.7
G6Sulfur [SSP5-8.5]	2020-2100	2	19.7

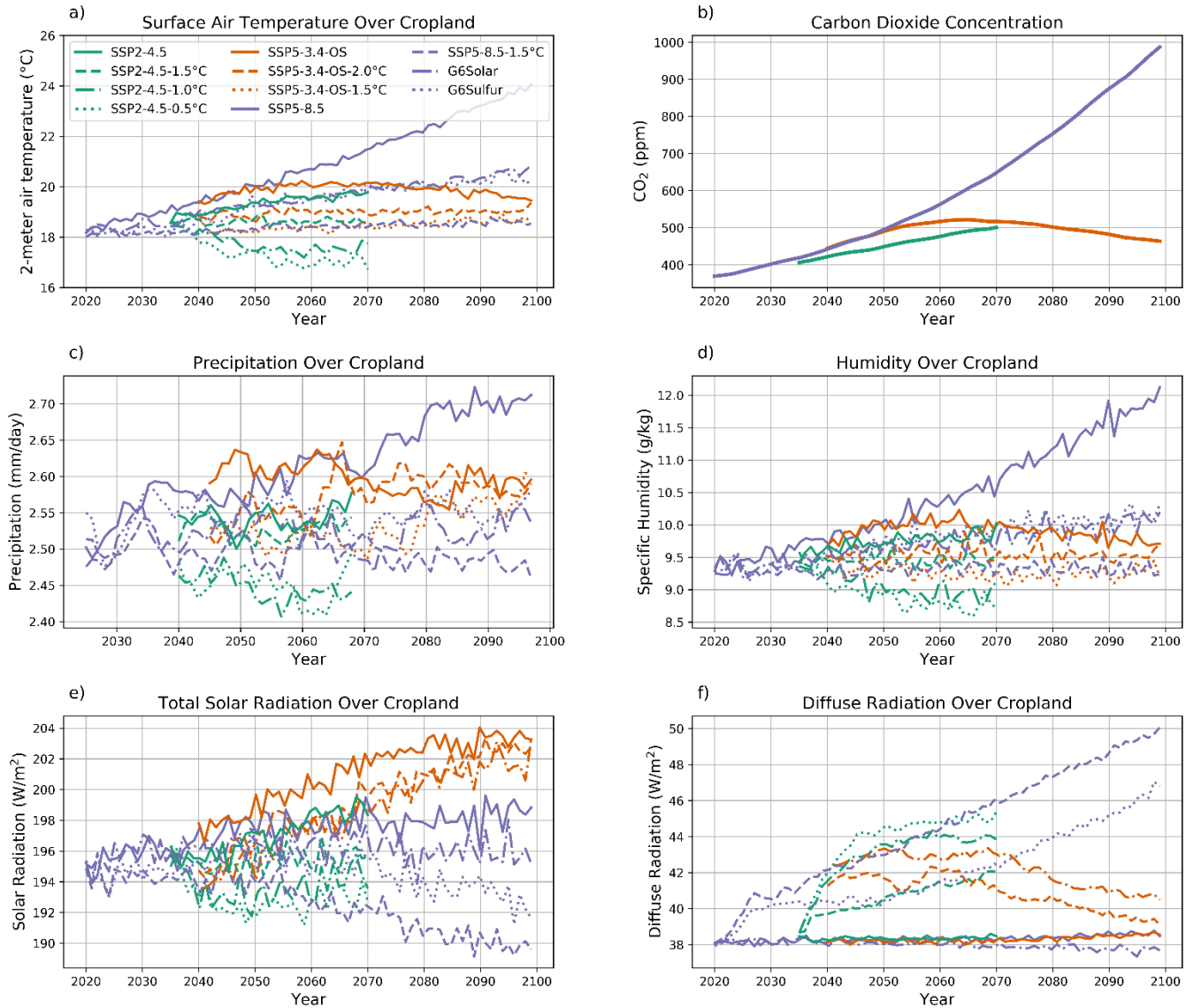


Figure 1. Global average time series of ensemble average temperature, carbon dioxide concentration, precipitation, specific humidity, total incoming solar radiation, and diffuse radiation over cropland for climate change and climate intervention scenarios. Precipitation is presented as a 5-year rolling average.

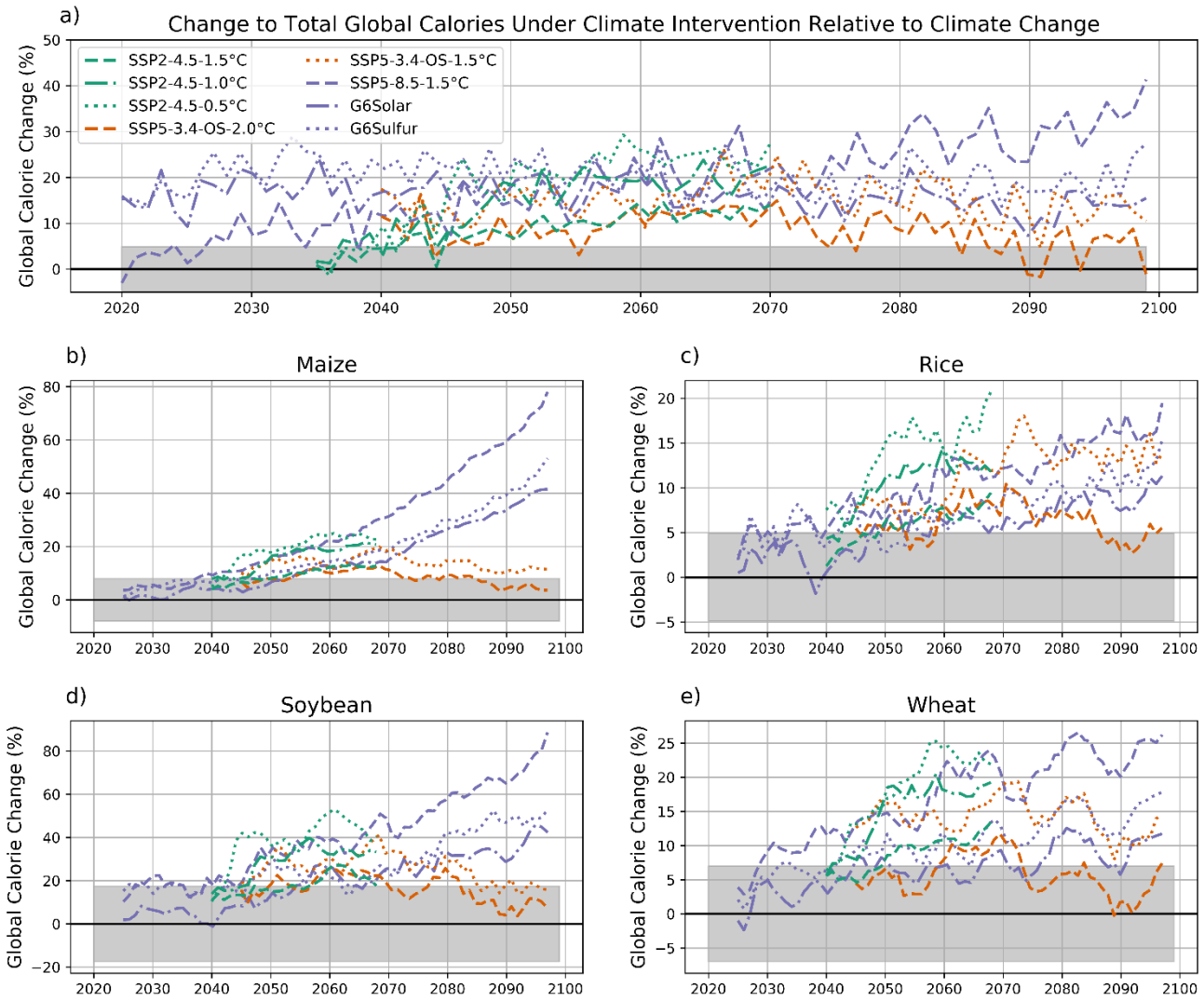


Figure 2. Time series of global percent change to a) total calories (maize, rice, soybean, and wheat), b) calories from maize, c) calories from rice, d) calories from soybean, and e) calories from wheat under climate intervention relative to the corresponding climate change scenario. Gray shaded regions indicate the standard deviation of a 50 year detrended historical period. Panels b-e are presented as 5-year rolling averages.

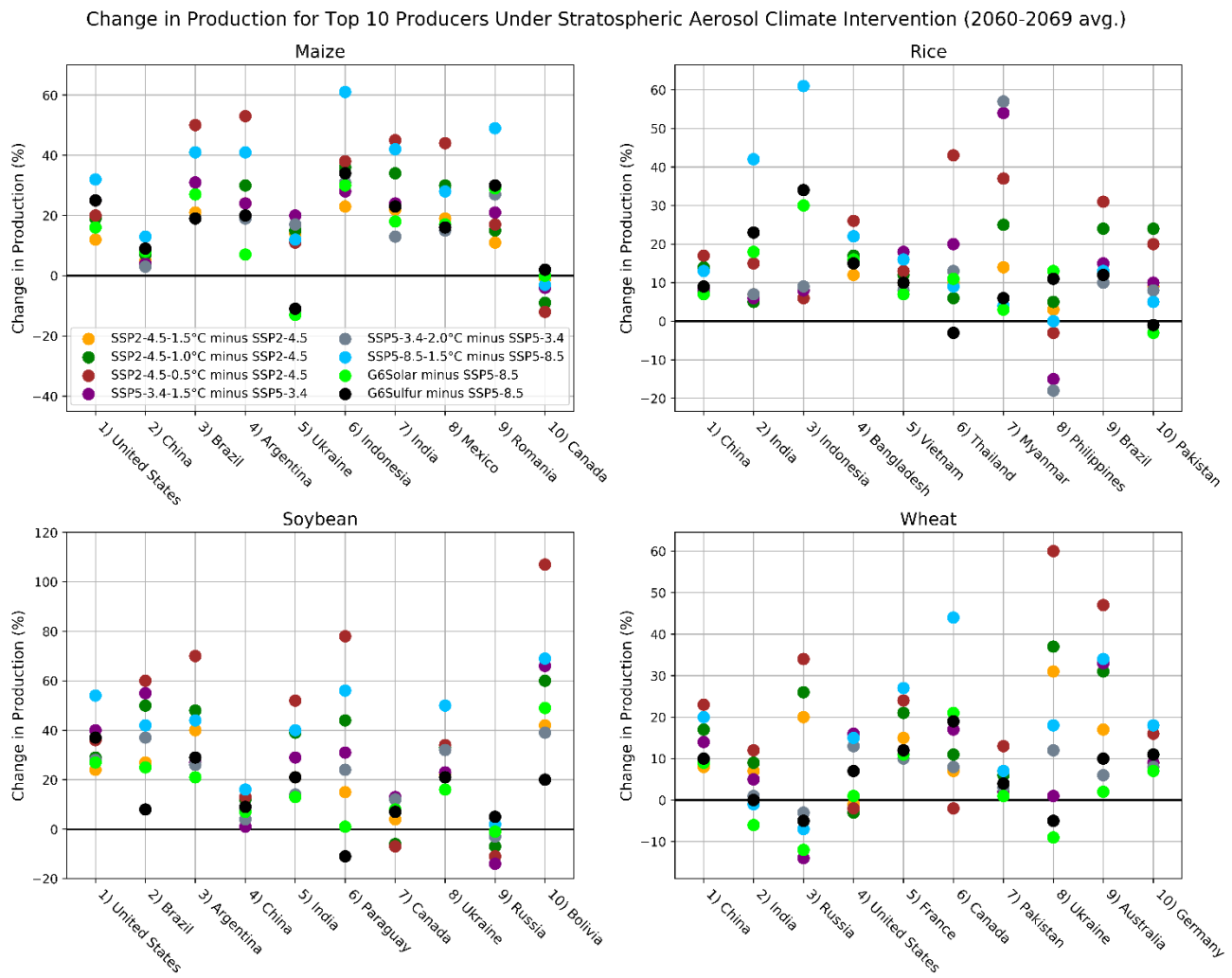


Figure 3. Percent change to maize, rice, soybean, and wheat production for the current FAOSTAT top 10 producers of each respective crop (2060-2069 average) under different climate intervention scenarios relative to climate change (FAO, 2022).

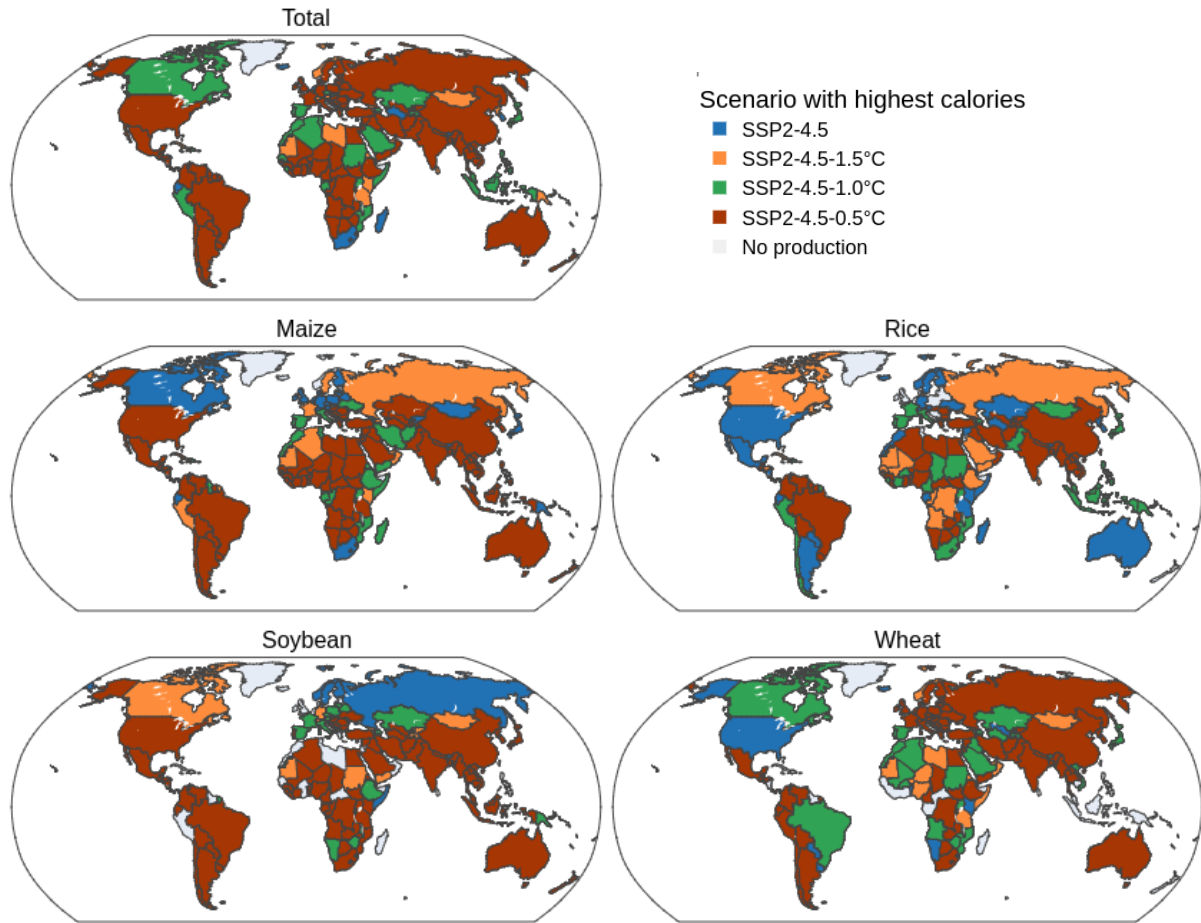


Figure 4. SSP2-4.5 scenarios that produces the highest calories from total crop production (maize + rice + soybean + wheat) and individual crops maize, rice, soybean, and wheat for each nation during the years 2060-2069.

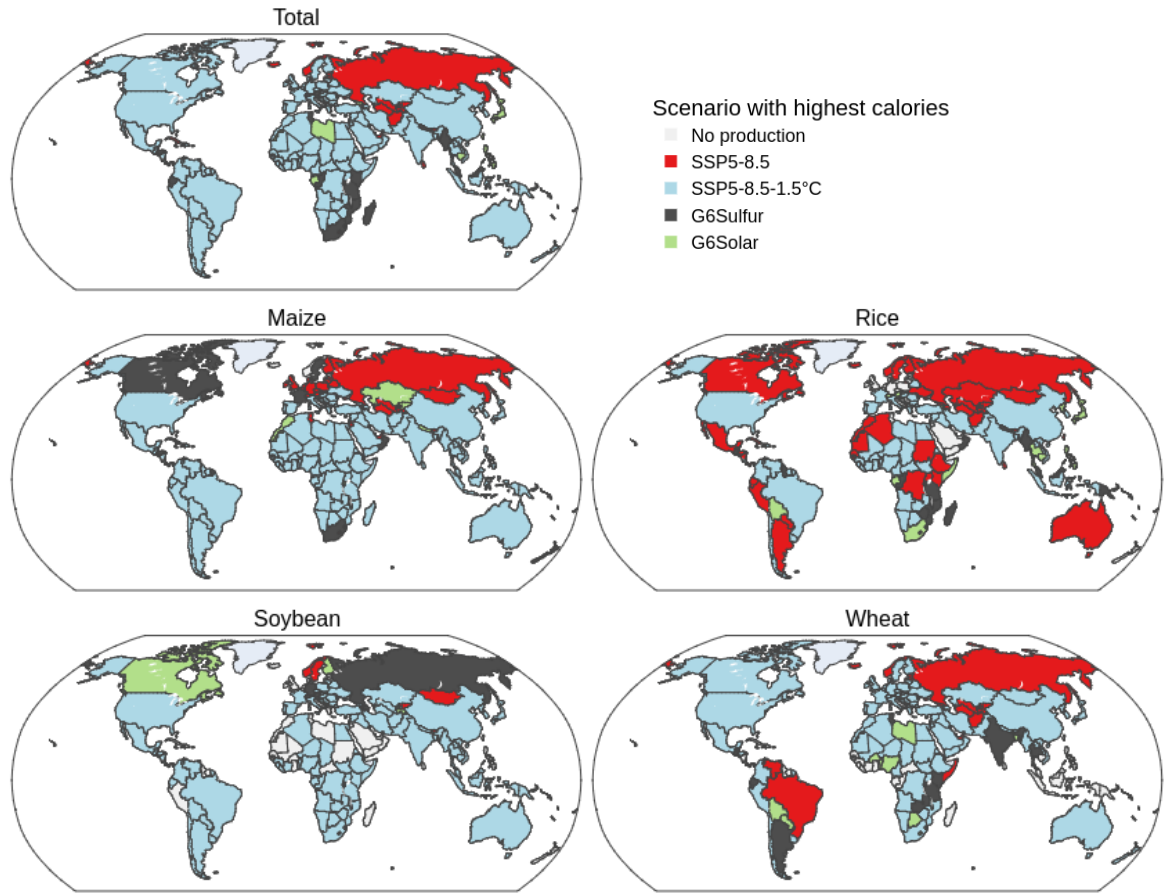


Figure 5. SSP5-8.5 scenarios that produces the highest calories from total crop production (maize + rice + soybean + wheat) and individual crops maize, rice, soybean, and wheat for each nation during the years 2060-2069.

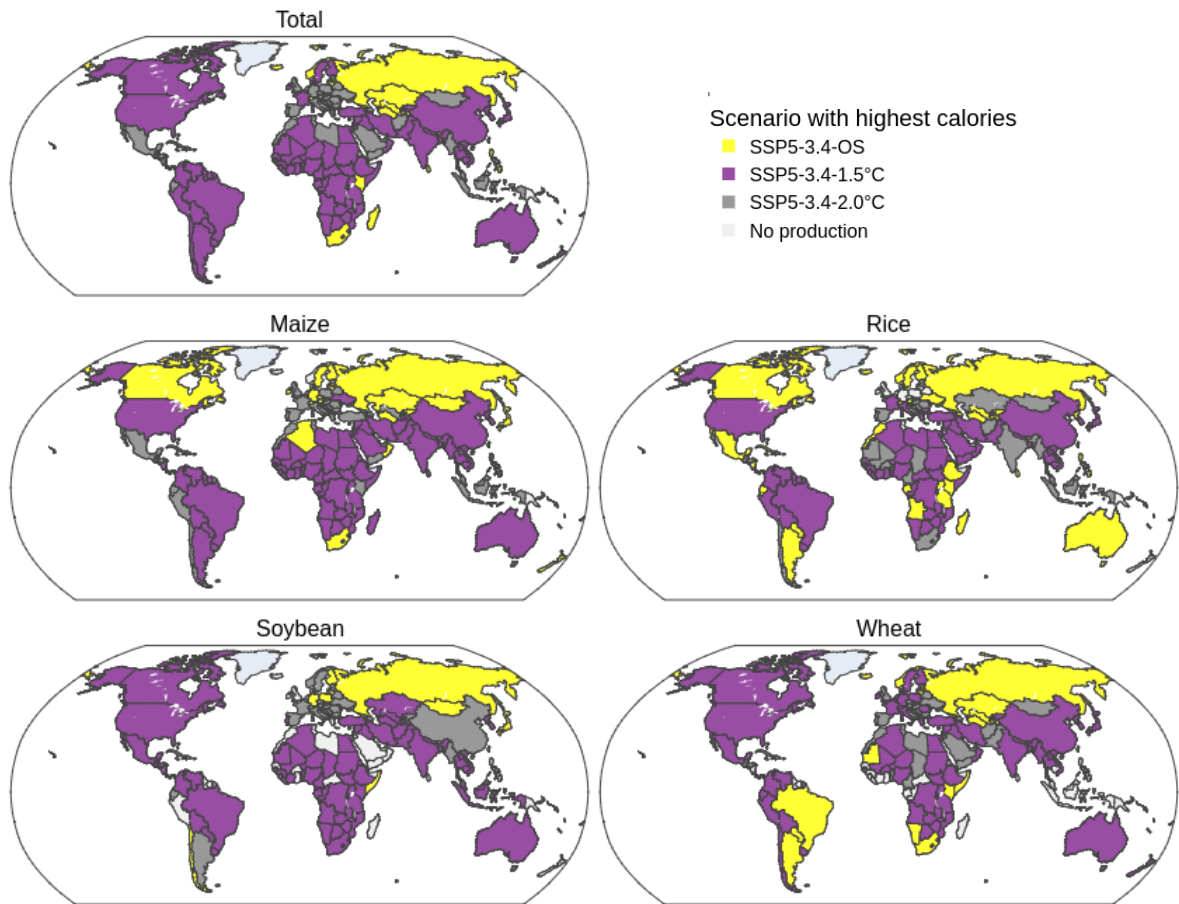


Figure 6. SSP5-3.4 scenarios that produces the highest calories from total crop production (maize + rice + soybean + wheat) and individual crops maize, rice, soybean, and wheat for each nation during the years 2060-2069.

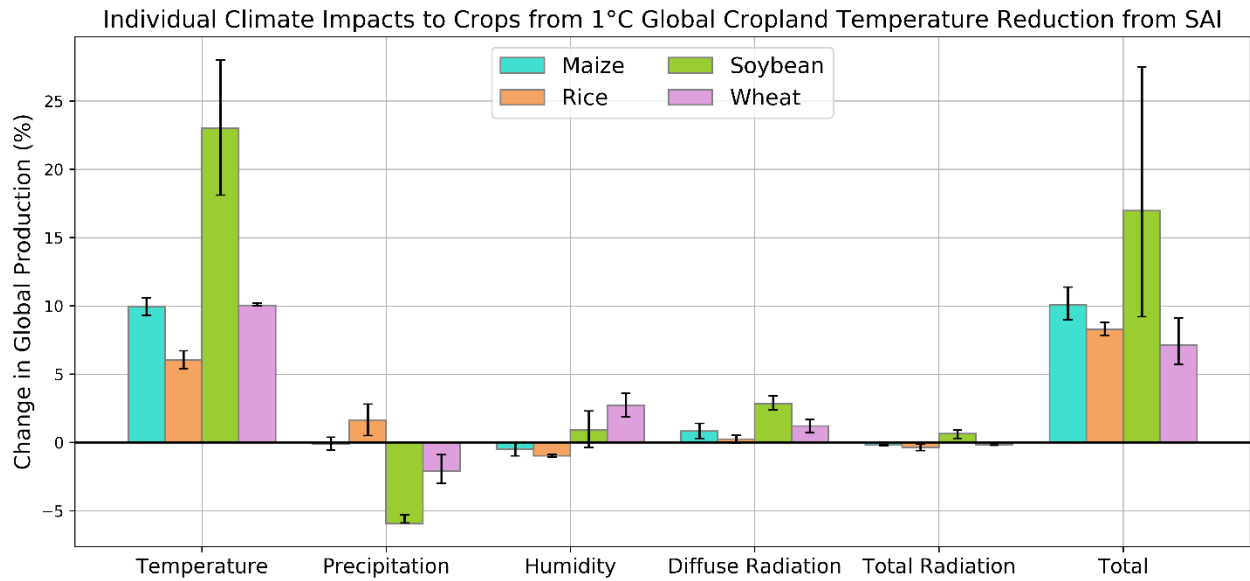


Figure 7. Individual contributions to global crop production changes under stratospheric aerosol climate intervention used to reduce global cropland temperatures by 1°C under SSP2-4.5-1.5°C relative to SSP2-4.5 during the years 2060-2069 (two ensemble member average). Error bars indicate ensemble range.

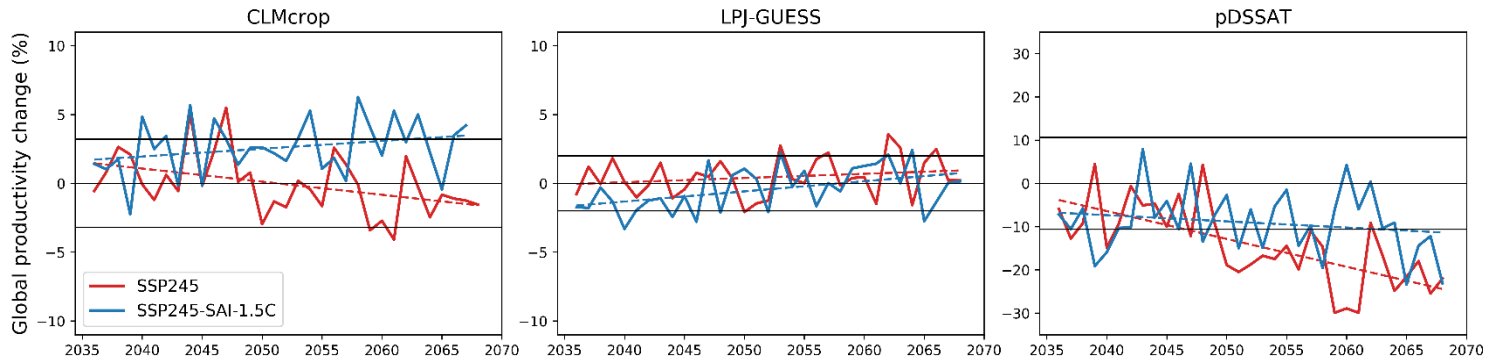


Figure 8. Time series of global maize production changes under the climate change scenario

SSP2-4.5 and the corresponding SAI scenario SSP2-4.5-SAI-1.5C relative to the reference

period of 2016-2025 for each of the three crop models CLM5crop, LPJ-GUESS, and pDSSAT.

Horizontal black lines indicate the standard deviation of production variability over the reference

period for each model. Colored dashed lines are trendlines of time series data for each scenario.

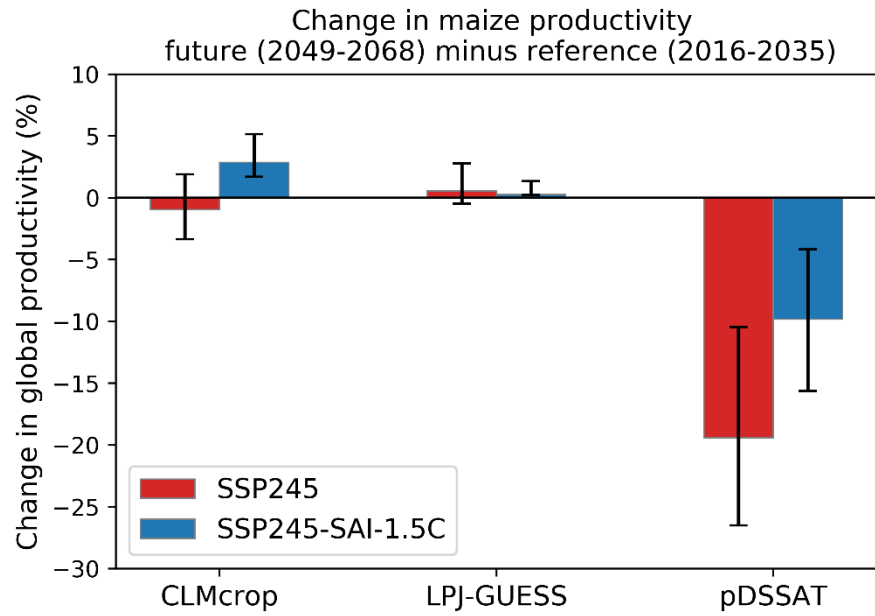


Figure 9. Percent change to global maize production in the three crop models under future (2049-2068 average) climate change and SAI relative to the reference period of 2016 to 2025. Error bars indicate the 25th and 75th percentiles of the data.

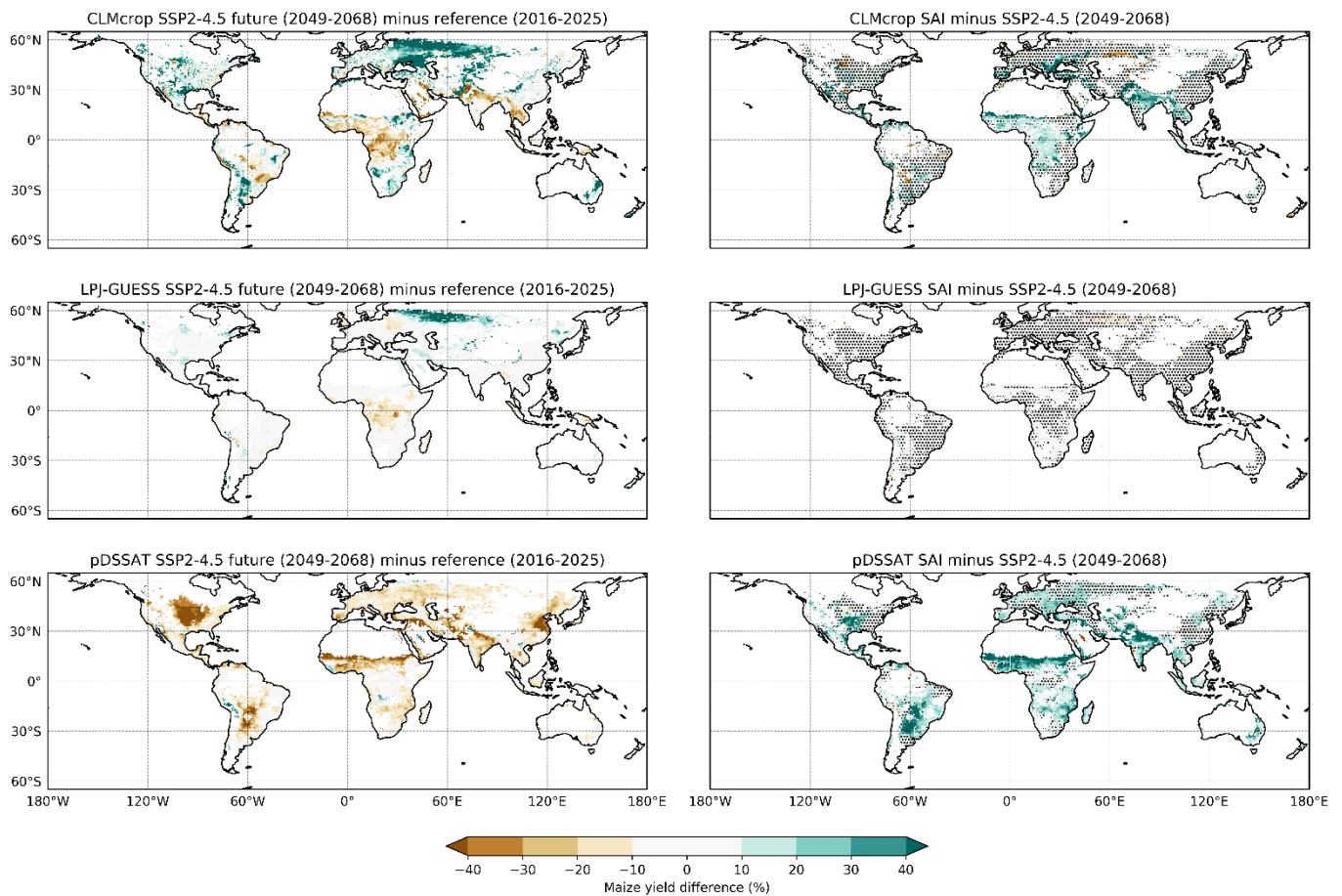


Figure 10. Relative maize yield difference between SSP2-4.5 future (2049-2068) minus reference (2016-2025) (left column) and SSP2-4.5-SAI-1.5C minus SSP2-4.5 averaged over the years 2049-2068 (right column). The left column plots correspond to the red lines and bars in Figures 1 and 2, and the right column plots correspond to the difference between the blue and red lines and bars in Figures 1 and 2. Stippled areas indicate grid cells where the difference is not statistically significant at the 95% confidence level based on a two-tailed Student's t-test.

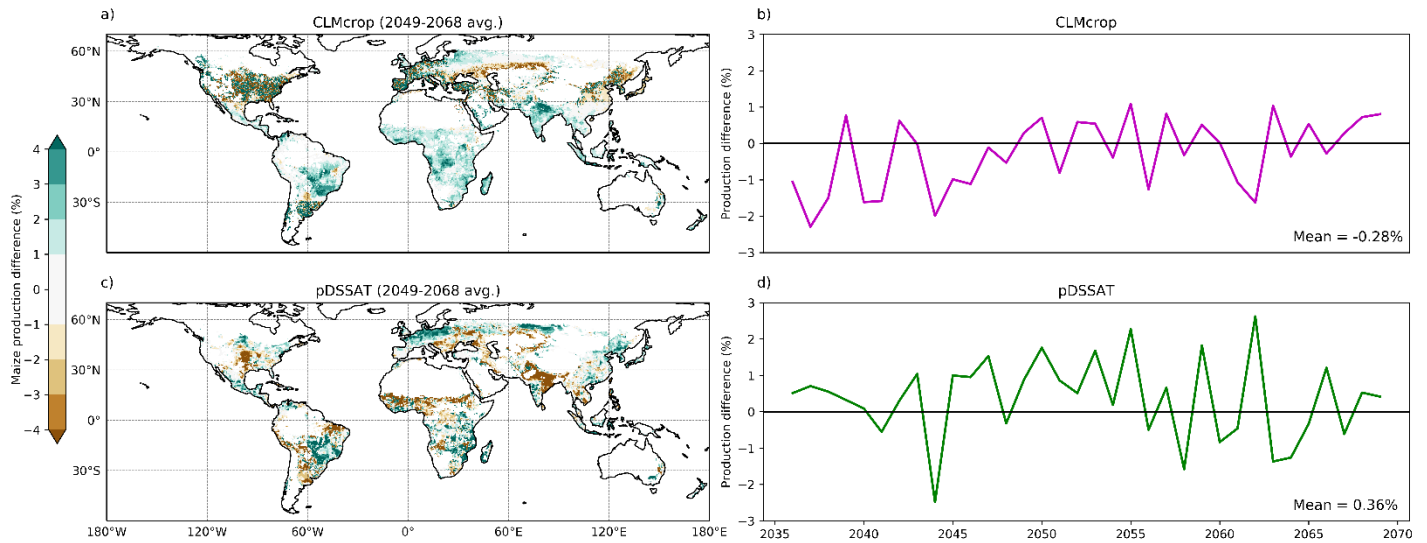


Figure 11. Maps of diffuse radiation impacts on global maize production in CLM5crop (a) and pDSSAT (c) over the years 2049-2068 and time series of diffuse radiation impacts on the sum of global maize production in CLM5crop (b) and pDSSAT (d) (SSP2-4.5-1.5C minus SSP2-4.5). For pDSSAT, this is calculated by comparing the differences between the SAI and climate change scenario with diffuse radiation data included and excluded. CLM5crop ran simulations that compared the impact of just changing the ratio of direct to diffuse radiation under SAI compared with the direct to diffuse ratio under climate change.

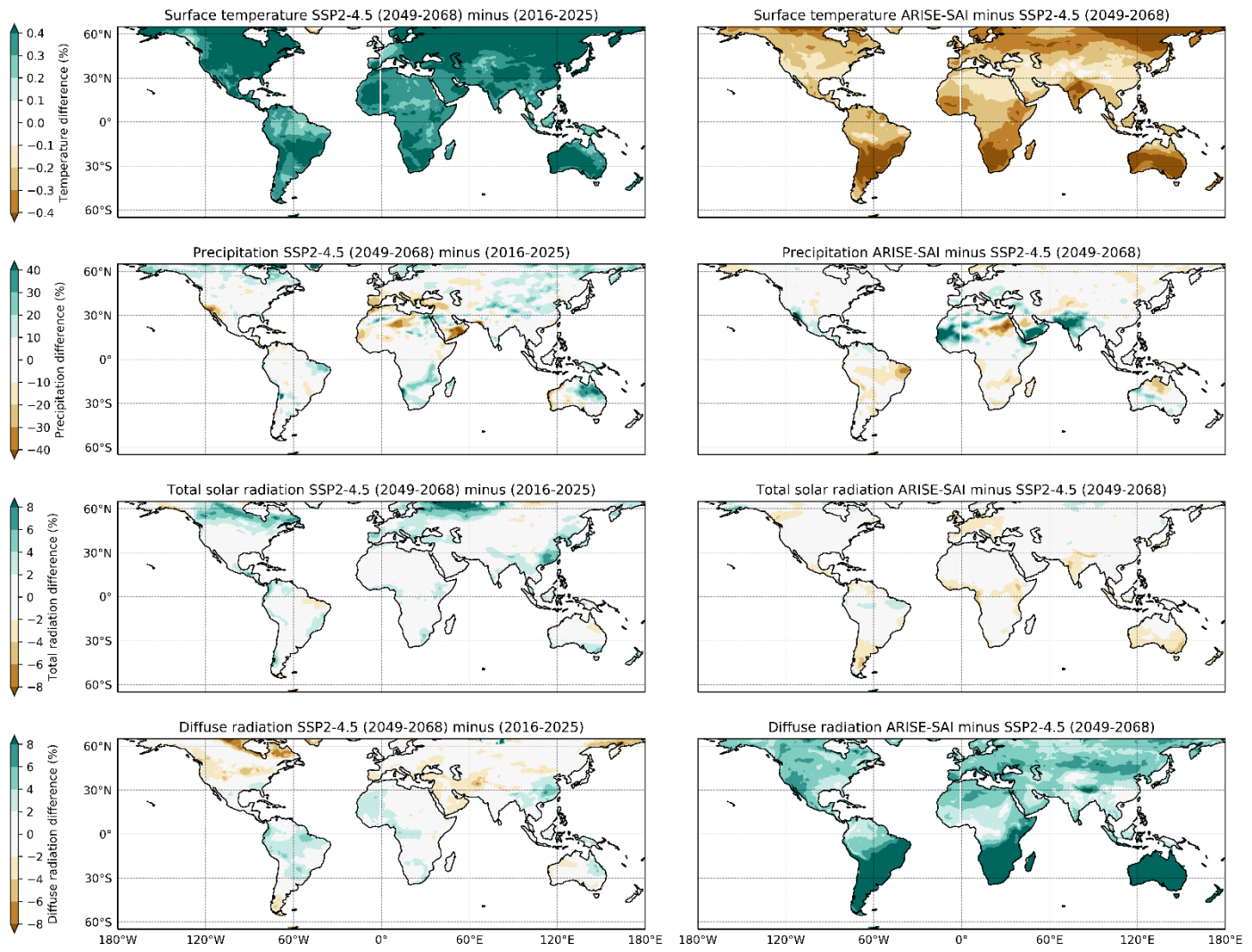


Figure 12. Maps of relative changes to temperature, precipitation, total radiation, and diffuse radiation under SSP2-4.5 future (2049-2068) minus SSP2-4.5 control (2016-2025) (left column) and SSP2-4.5-ARISE-SAI minus SSP2-4.5 (2049-2068) (right column) as simulated by CESM2-WACCM6 (Richter et al., 2022).

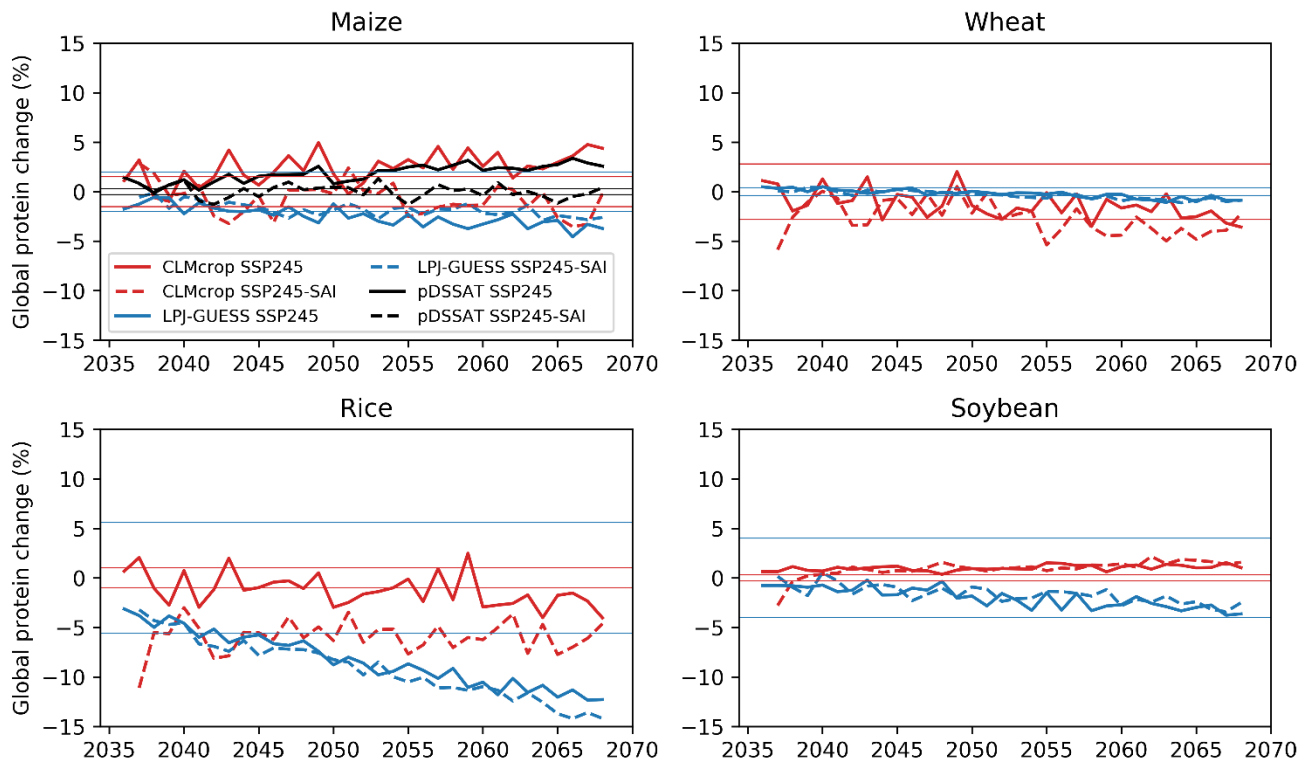


Figure 13. The annual time series of changes to global average crop protein content (Grain N:C) for maize, rice, soybean, and wheat as simulated by CLMcrop, LPJ-GUESS, and pDSSAT under SSP2-4.5 and SAI relative to the reference period (2016-2025). Horizontal lines indicated +/- one standard deviation of crop protein under the reference period for each model and crop.

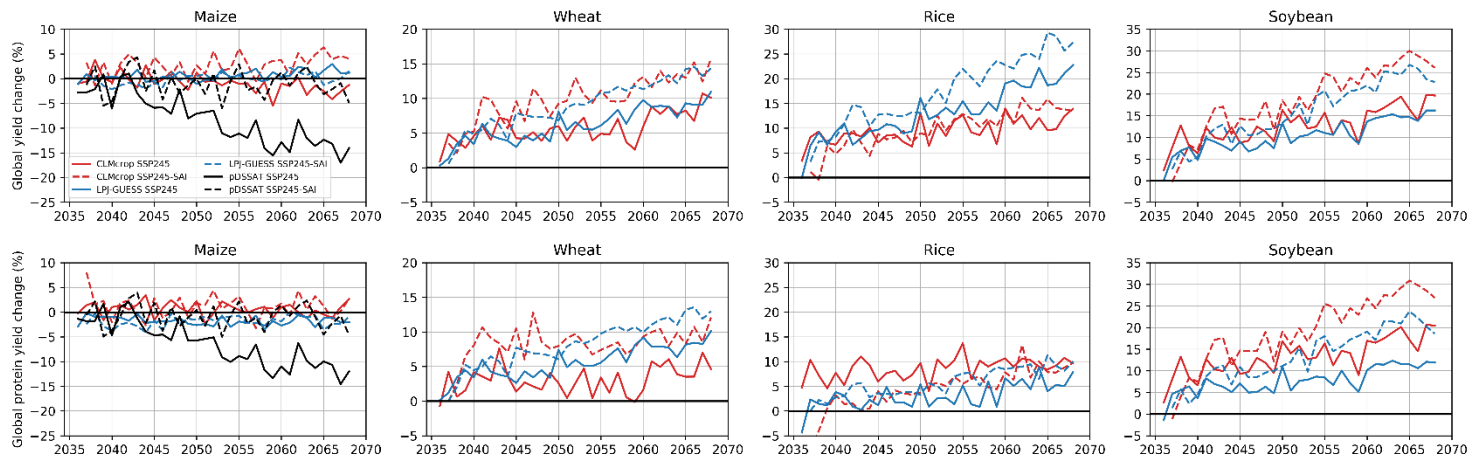


Figure 14. Time series of changes to global average yield under climate change and SAI relative to the reference period (2016-2025) for each crop model (top). Time series of changes to global average protein yield changes under climate change and SAI (bottom).

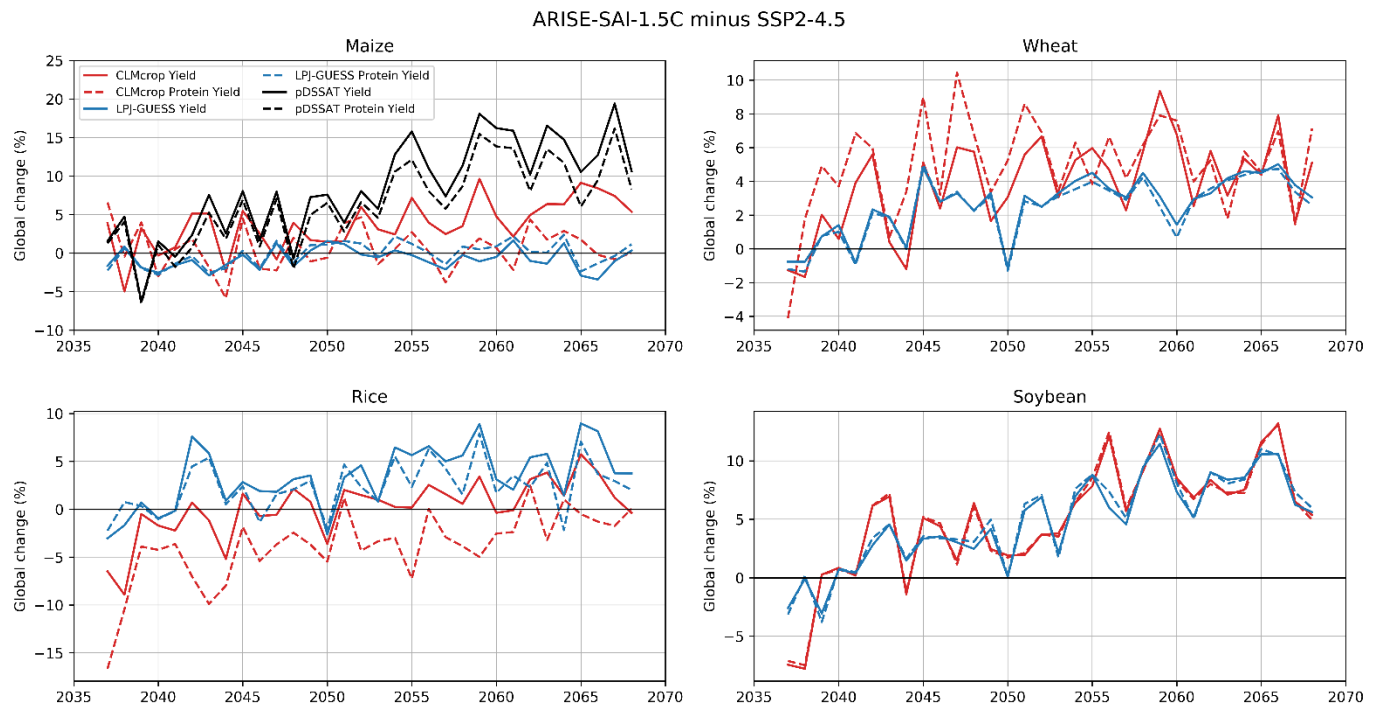


Figure 15. Time series of changes to global average yield and protein yield under SAI minus SSP2-4.5 for CLMcrop, LPJ-GUESS, and pDSSAT.

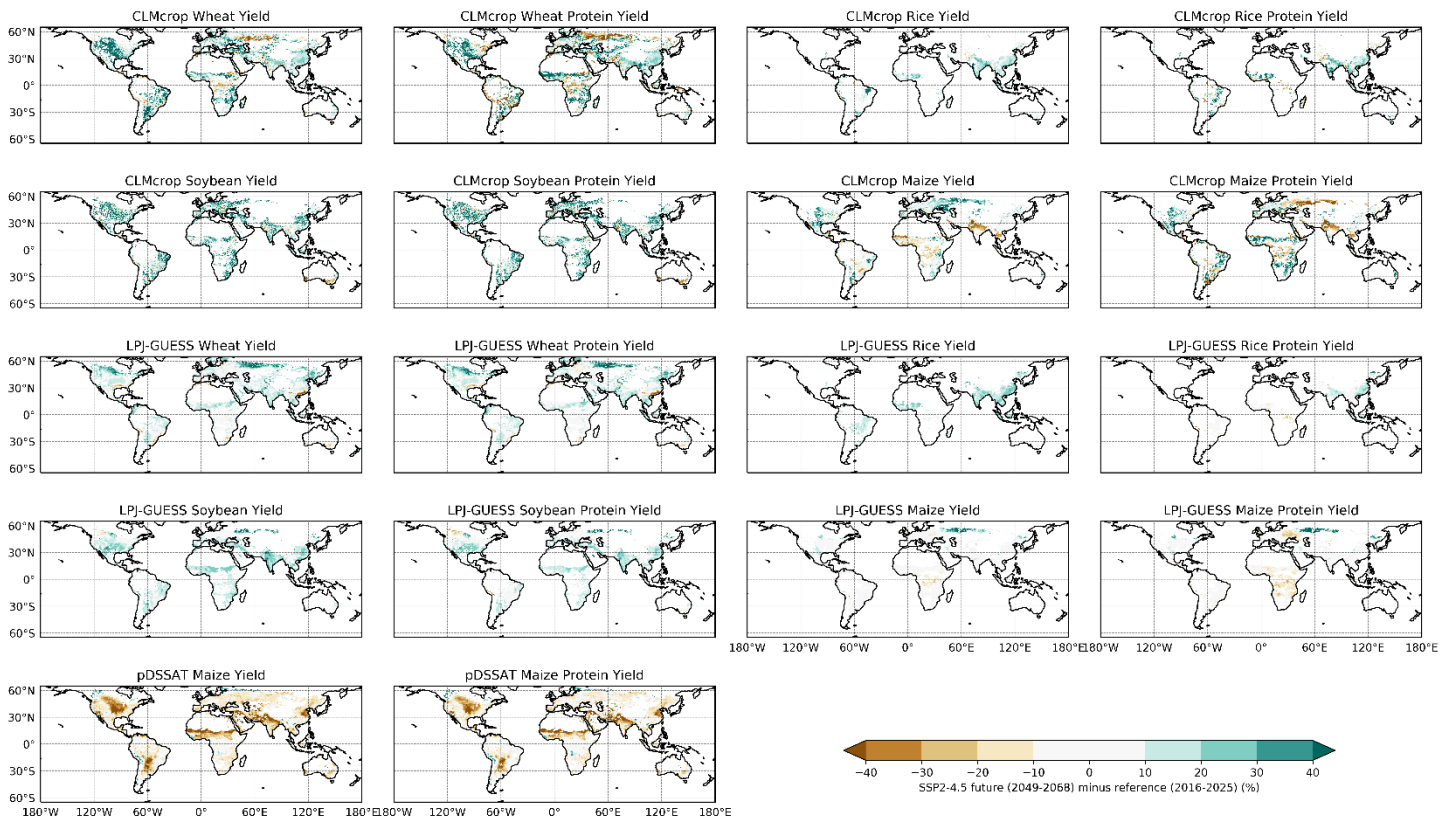


Figure 16. Changes to global yields and protein yields under future climate change (2049-2069) relative to the reference period of 2016-2025 for CLMcrop, LPJ-GUESS, and pDSSAT.

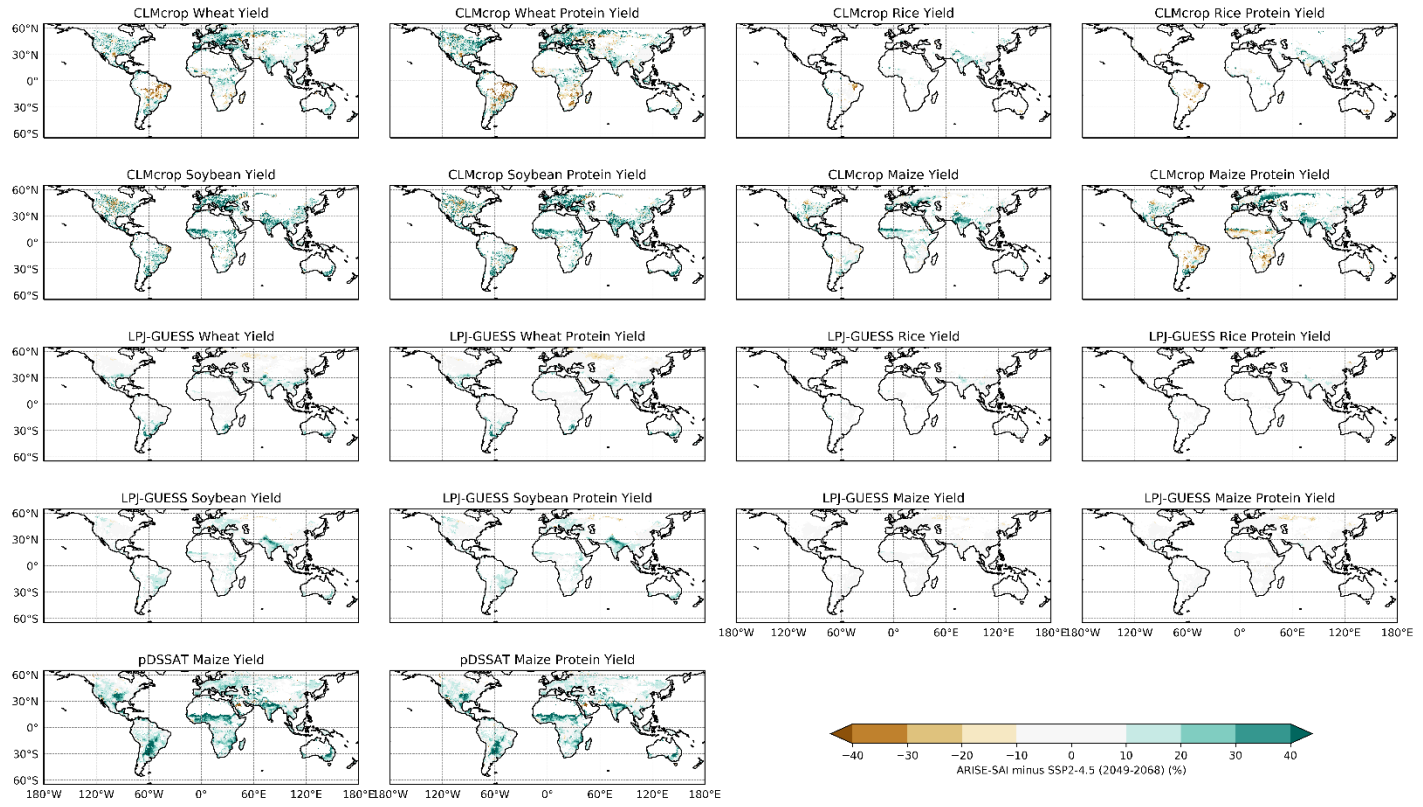


Figure 17. Changes to global yields and protein yields under future SAI (2049-2069) minus climate change (2049-2068) for CLMcrop, LPJ-GUESS, and pDSSAT.

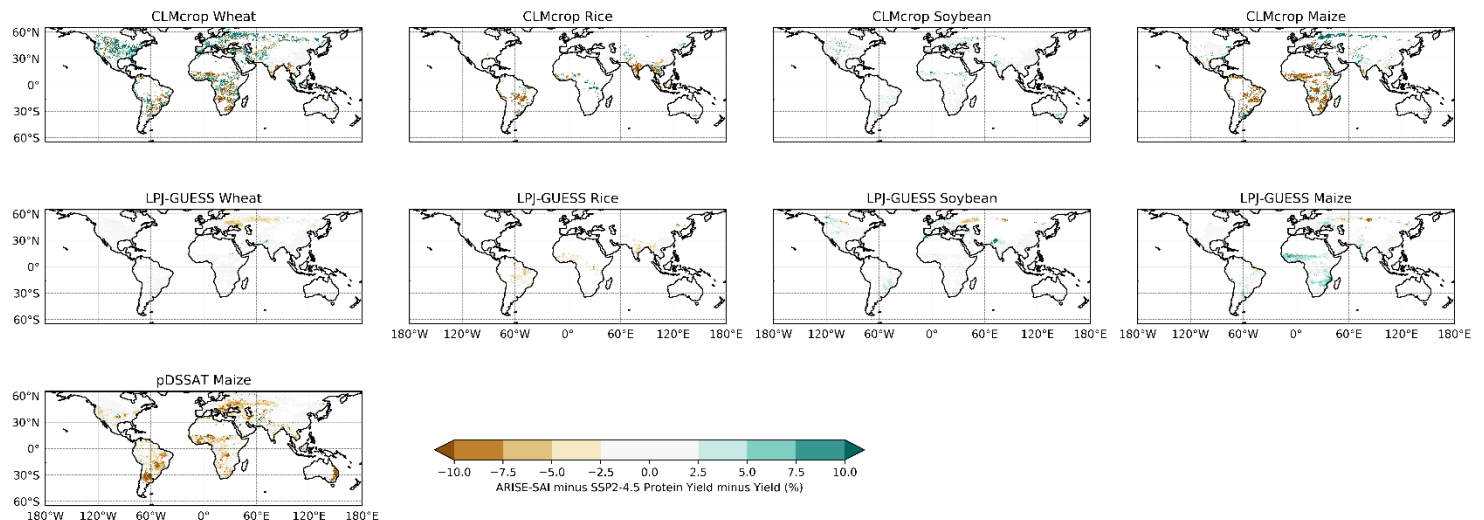
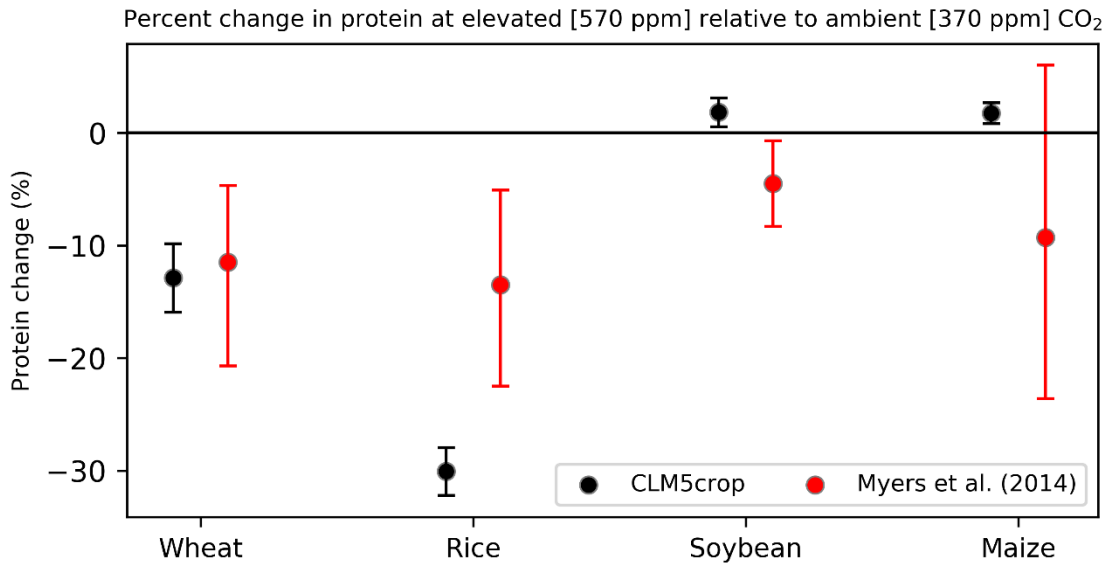
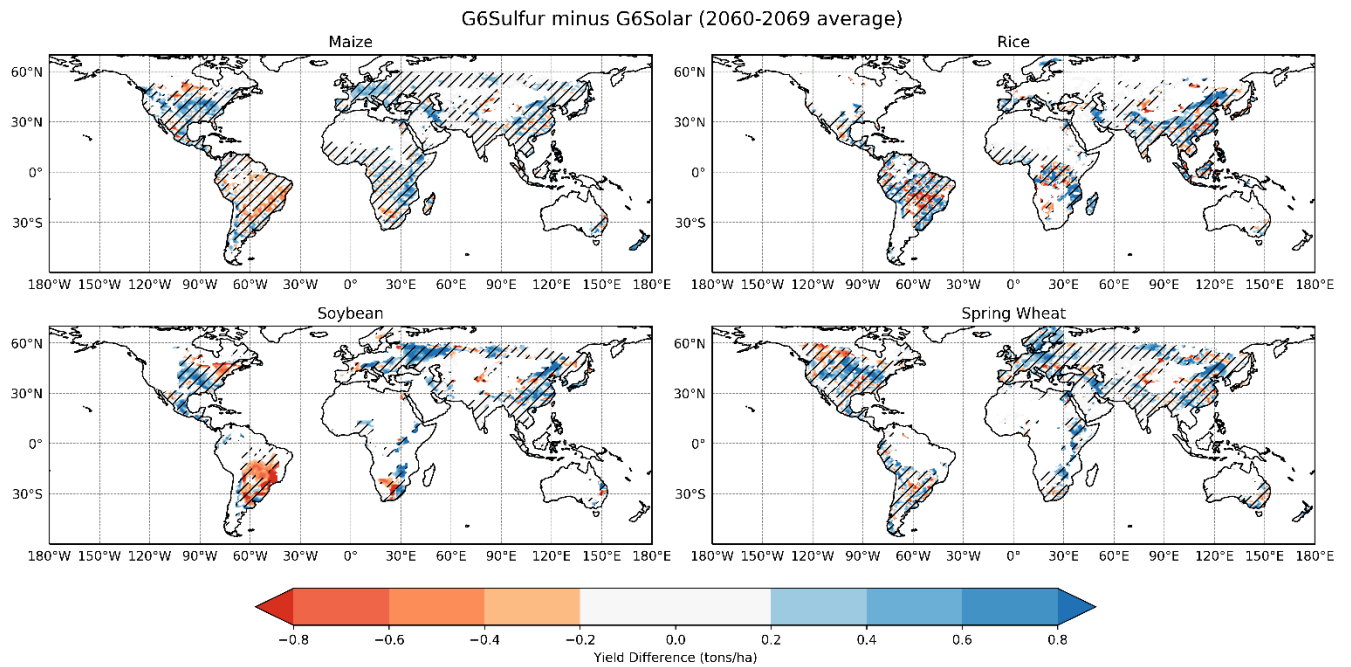


Figure 18. [SAI minus SSP2-4.5 (protein yield)] minus [SAI minus SSP2-4.5 (yield)] during years 2049-2068. This is subtracting the “protein yield” from the “yield” panels in Figure 6.

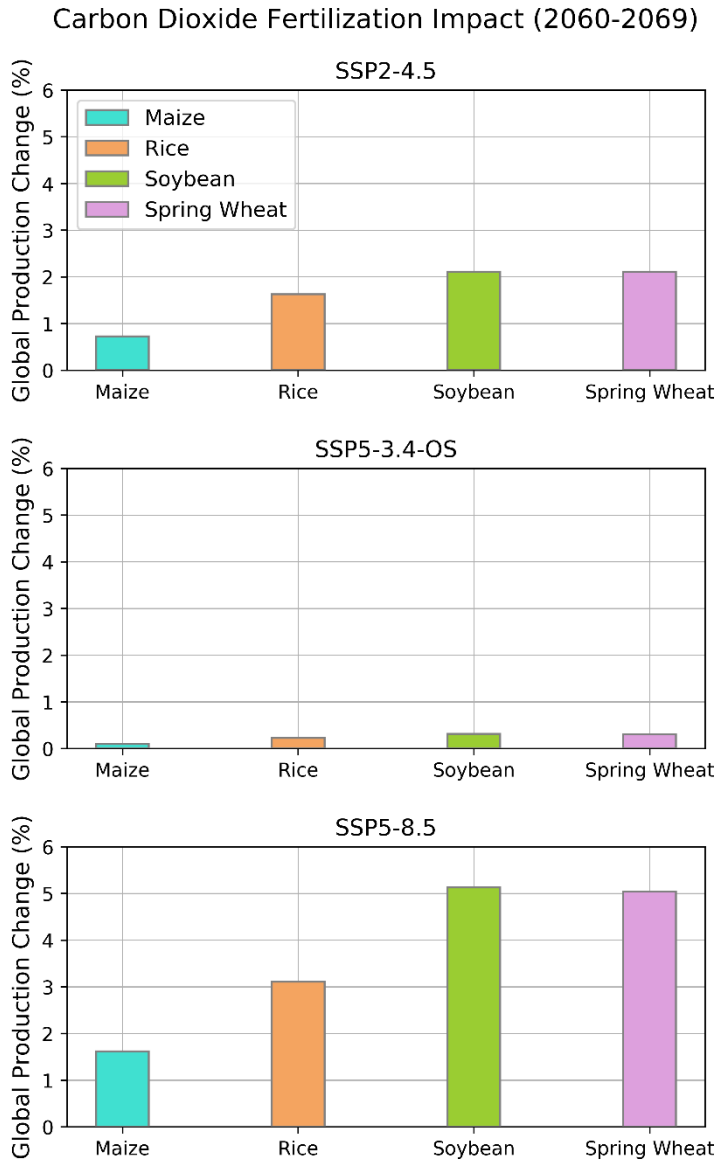
Section 9.0: Supplementary Figures



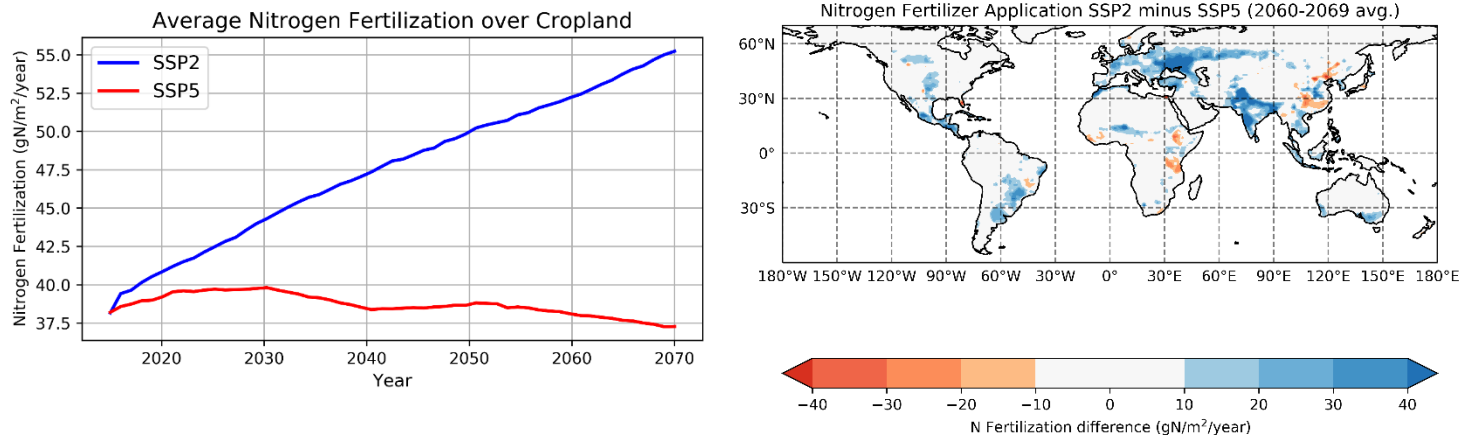
Supplementary Figure 1. Relative protein change from elevated CO₂ in CLM5crop for wheat (masked over Australia), rice (masked over Japan), soybean (masked over United States), and maize (masked over United States). Masked locations follow Myers et al. (2014). Atmosphere forcing for CLM5crop was from years 2016-2020 of SSP2-4.5 CESM2 output for both the elevated and ambient scenarios. Error bars for CLM5crop represent the standard deviation of interannual protein changes for each crop during this 5-year period. Myers et al. (2014) values represent the mean protein change across cultivars, with error bars representing the 95% confidence interval range across cultivars.



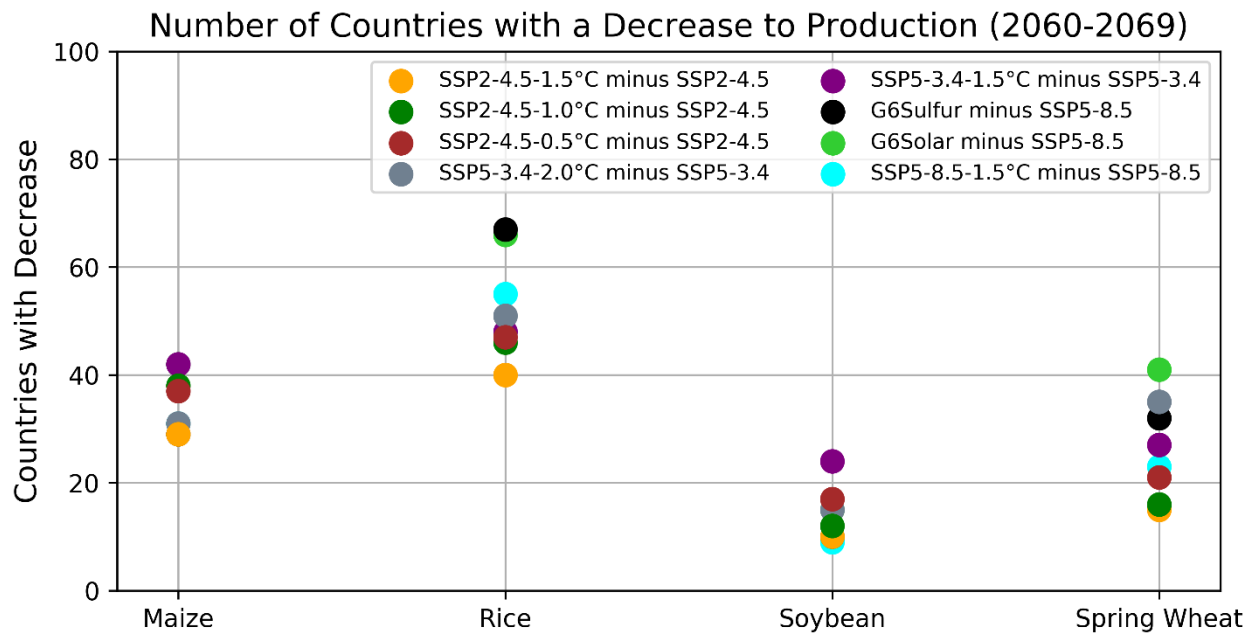
Supplementary Figure 2. Regional differences in yield between G6sulfur and G6Solar averaged over the years 2060-2069. Hatched areas are insignificant at the 95% confidence level (p -value > 0.05) based on a two-tailed Student's t -test.



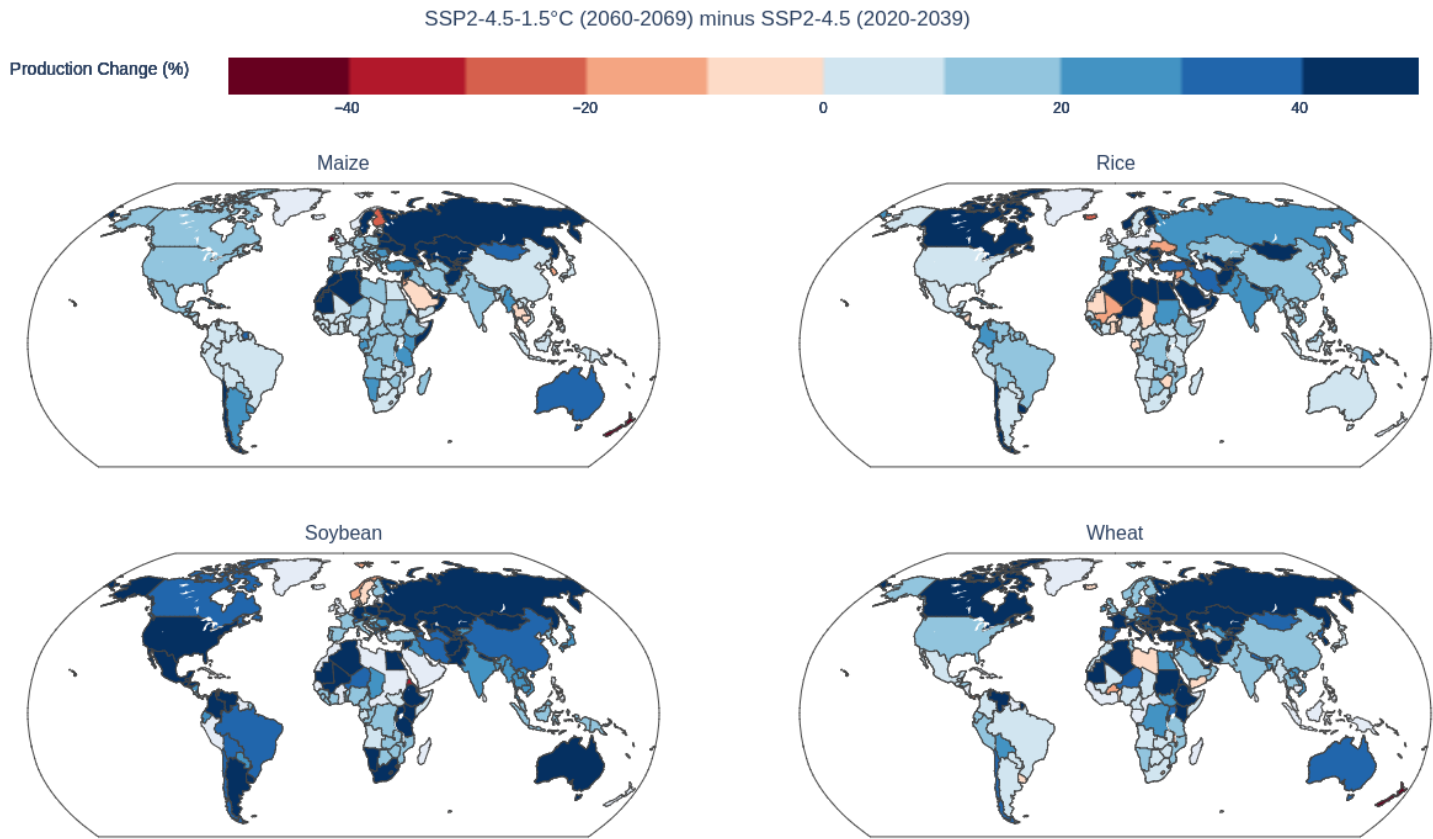
Supplementary Figure 3. Average impact of increased CO₂ from 2060-2069 on maize, rice, soybean, and wheat under SSP2-4.5, SSP5-3.4-OS, and SSP5-8.5 relative to constant CO₂ from 2060.



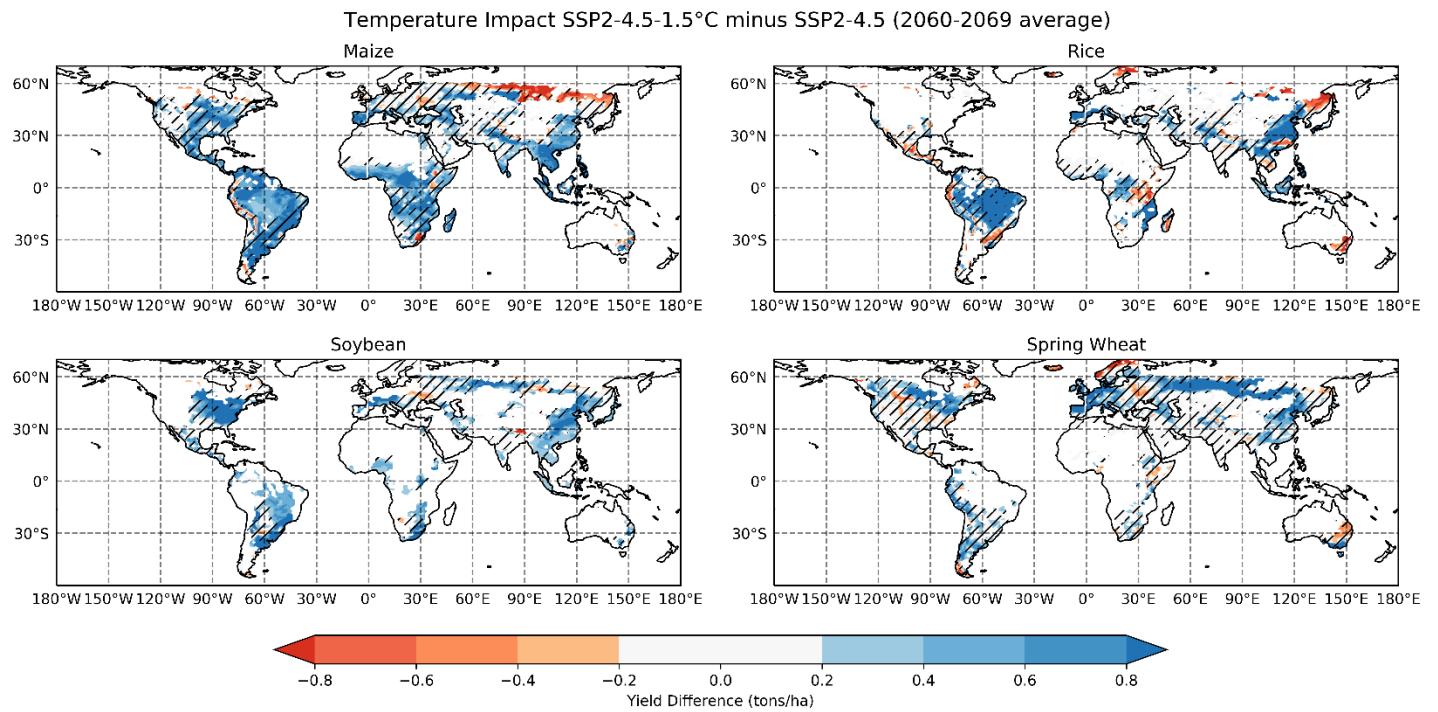
Supplementary Figure 4. Average nitrogen fertilizer applied to cropland under SSP2 and SSP5 during the years 2015-2070.



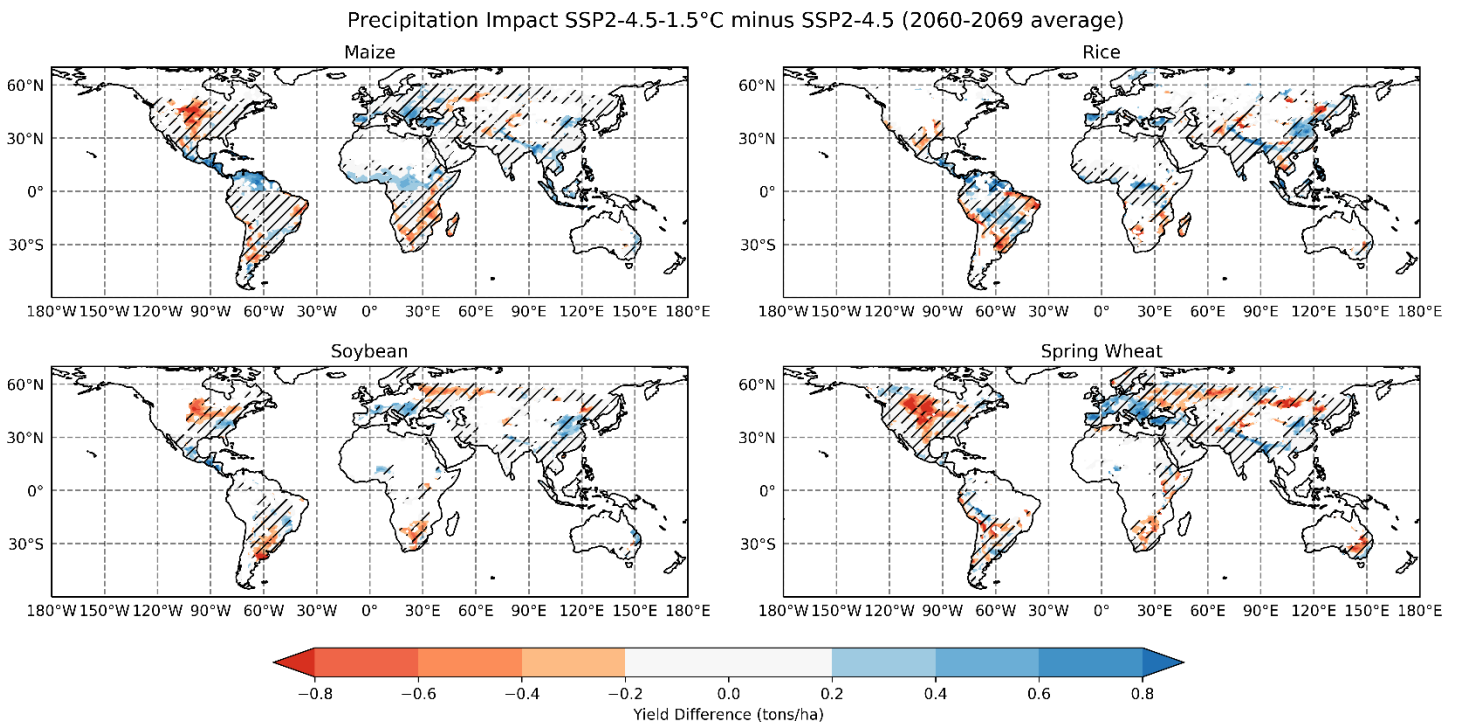
Supplementary Figure 5. The number of nations that show a decrease to their production of maize, rice, soybean, or spring wheat under SAI relative to climate change averaged over the years 2060-2069.



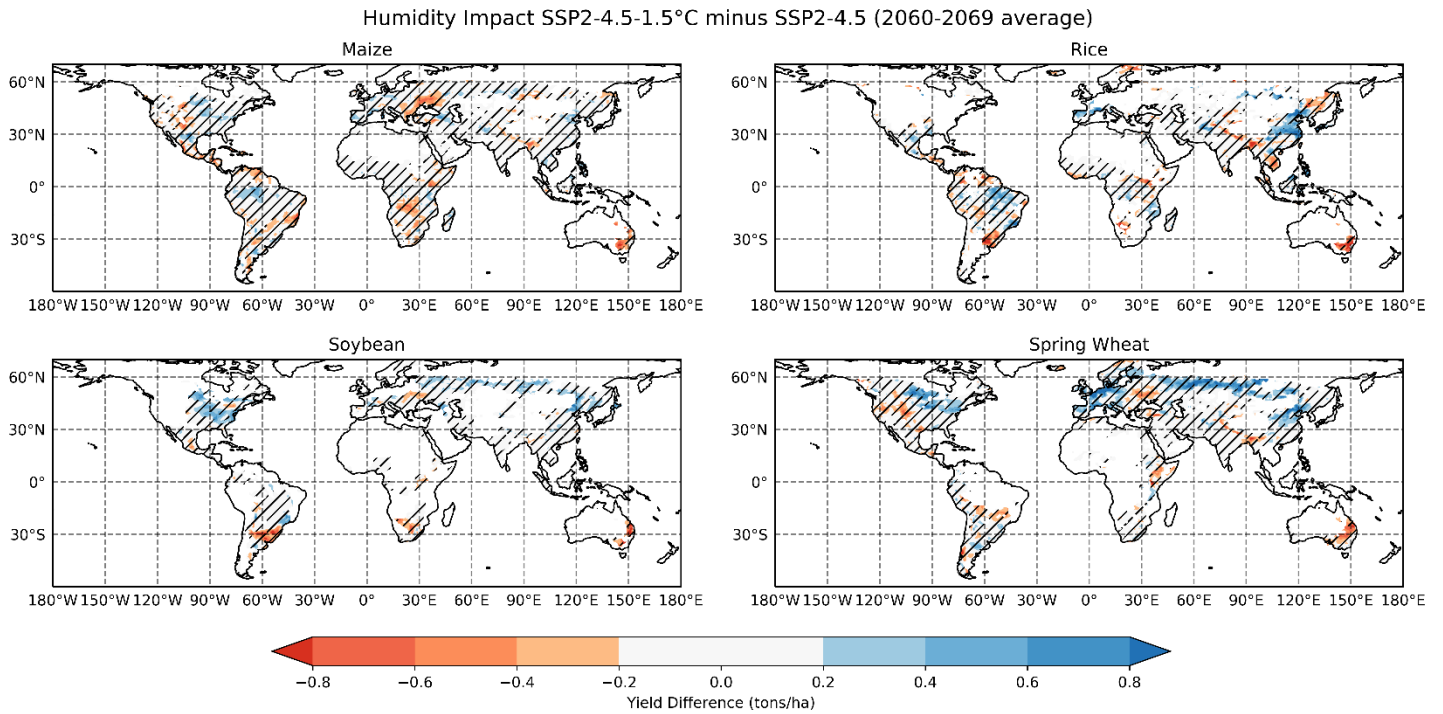
Supplementary Figure 6. The percentage change to production for each nation for each crop under SSP2-4.5-1.5°C (2060-2069 average) minus SSP2-4.5 (2020-2039 average).



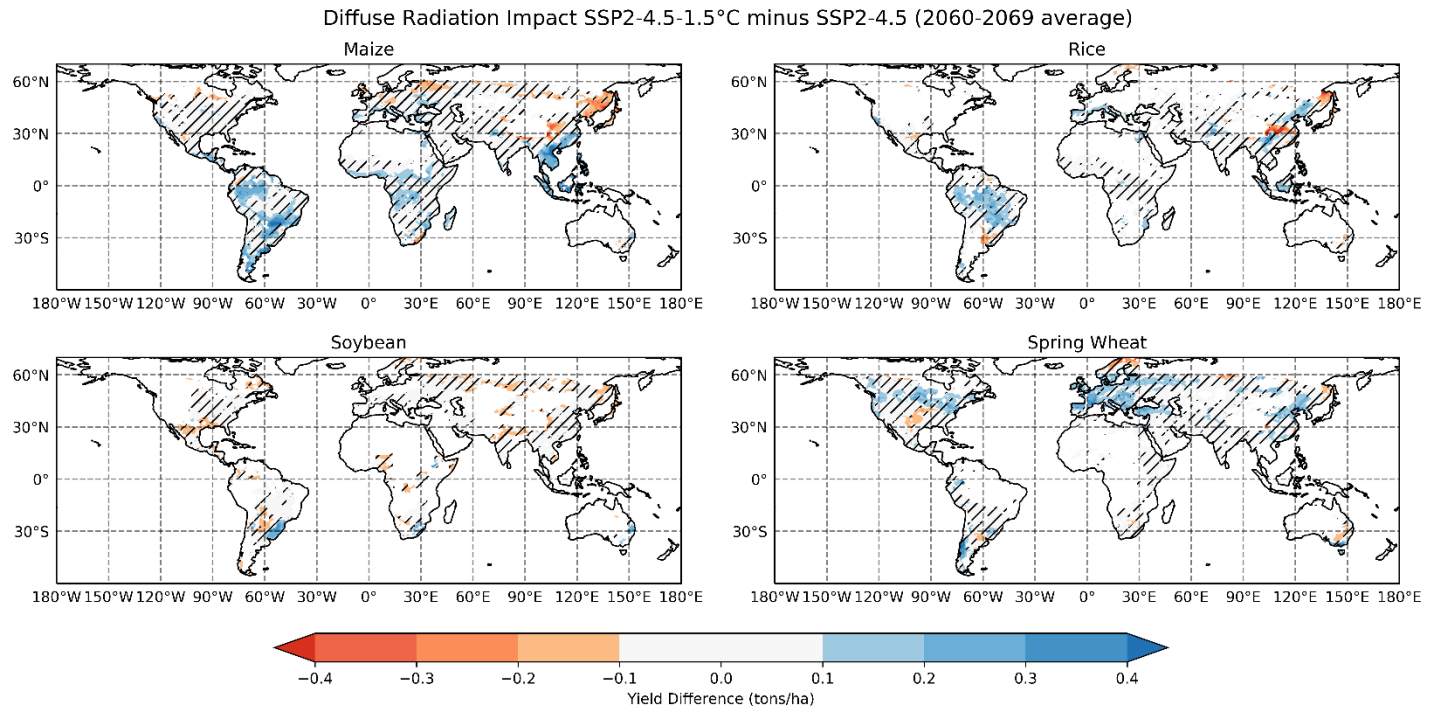
Supplementary Figure 7. Temperature impact on yield under SSP2-4.5-1.5°C minus SSP2-4.5 average from 2060-2069. Hatched areas are insignificant at the 95% confidence level (p -value > 0.05) based on a two-tailed Student's t -test.



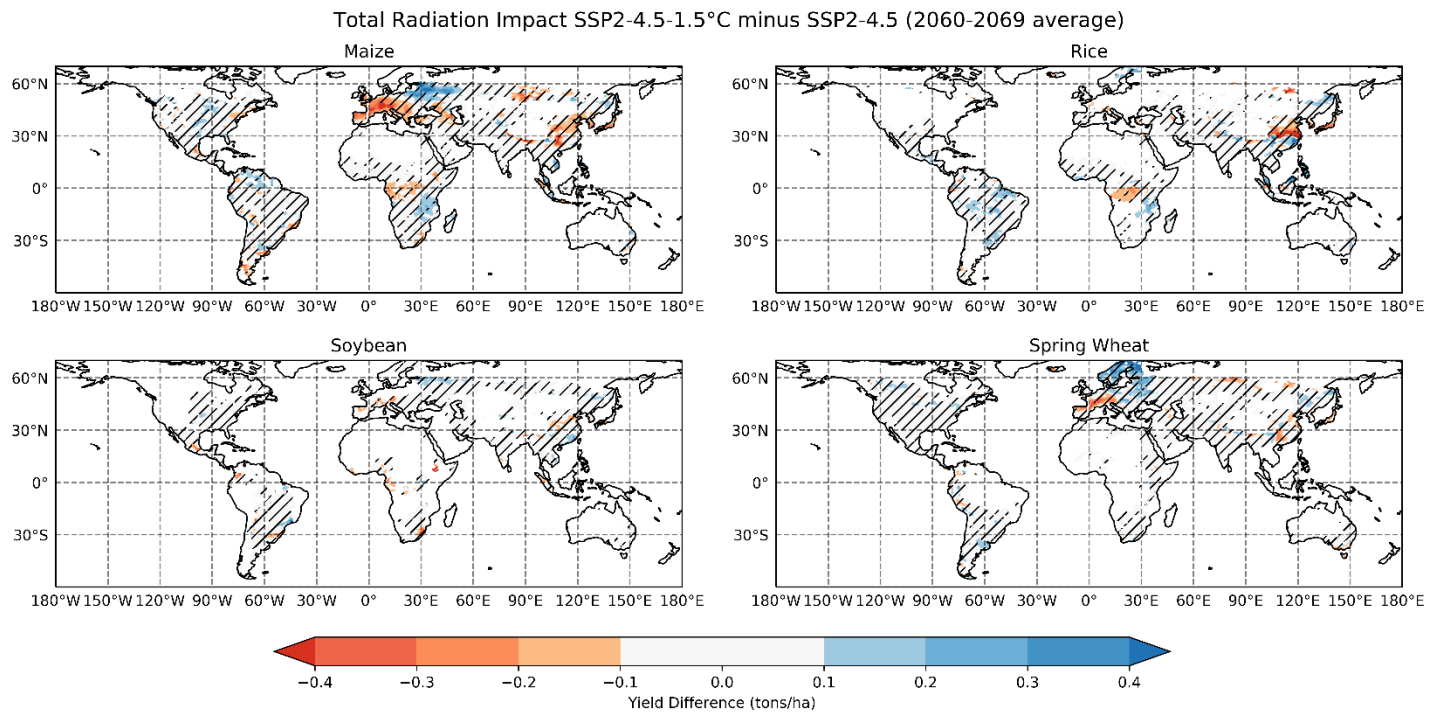
Supplementary Figure 8. Precipitation impact on yield under SSP2-4.5-1.5°C minus SSP2-4.5 average from 2060-2069. Hatched areas are insignificant at the 95% confidence level (p -value > 0.05) based on a two-tailed Student's t -test.



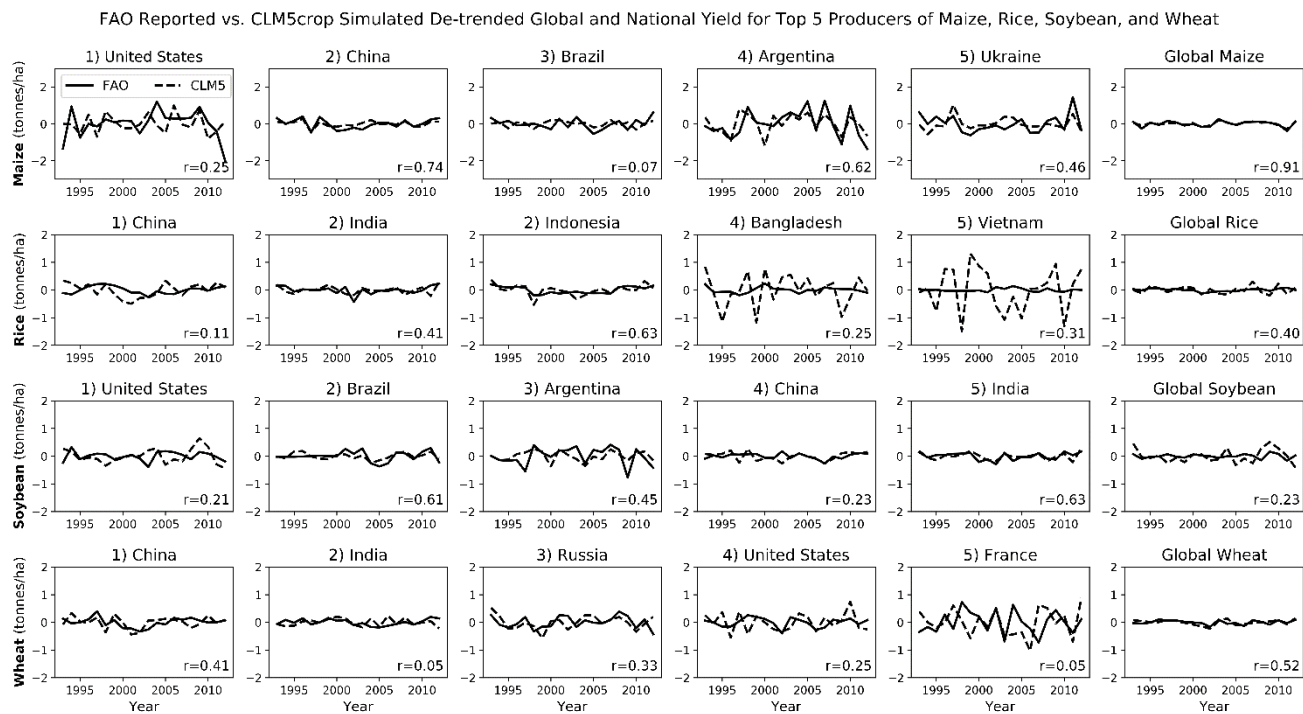
Supplementary Figure 9. Specific humidity impact on yield under SSP2-4.5-1.5°C minus SSP2-4.5 average from 2060-2069. Hatched areas are insignificant at the 95% confidence level (p -value > 0.05) based on a two-tailed Student's t -test.



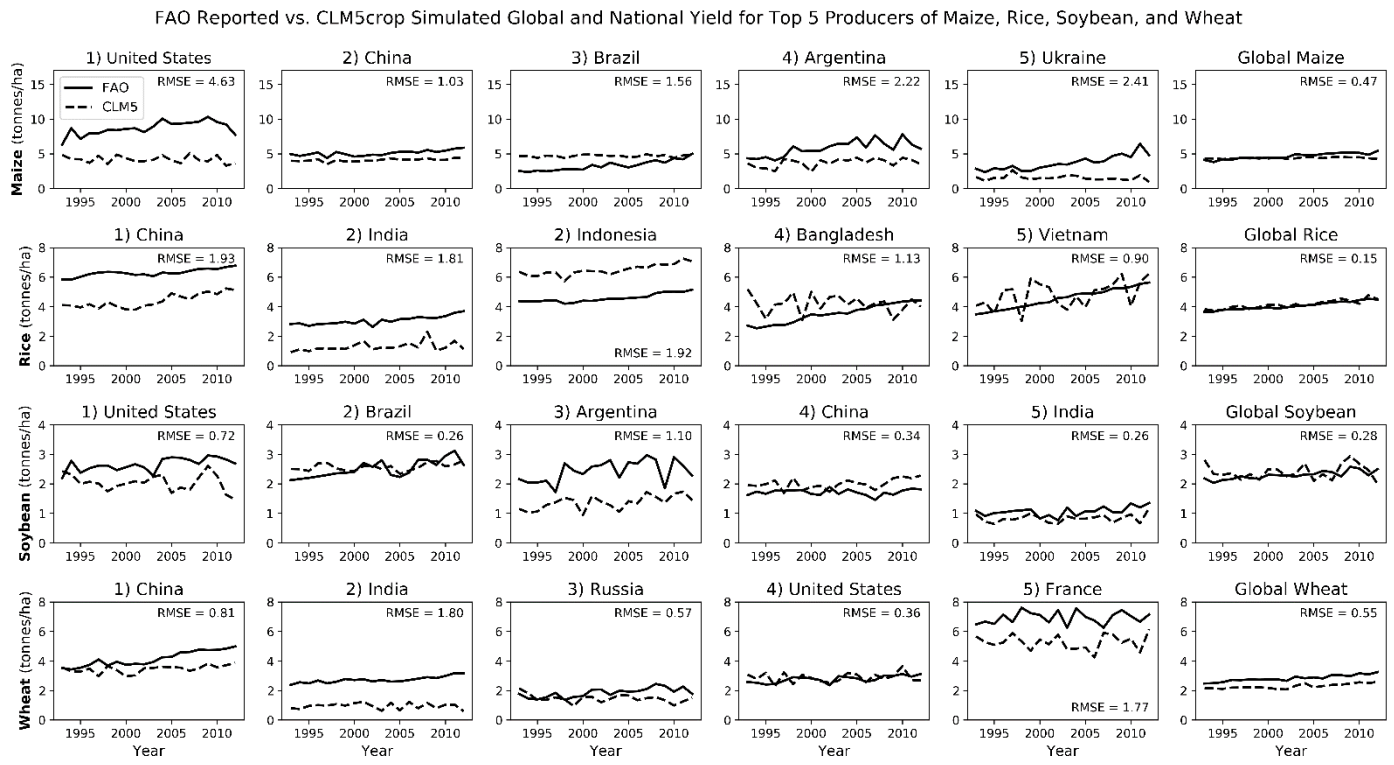
Supplementary Figure 10. Diffuse radiation impact on yield under SSP2-4.5-1.5°C minus SSP2-4.5 average from 2060-2069. Hatched areas are insignificant at the 95% confidence level (p -value > 0.05) based on a two-tailed Student's t -test.



Supplementary Figure 11. Total radiation impact on yield under SSP2-4.5-1.5°C minus SSP2-4.5 average from 2060-2069. Hatched areas are insignificant at the 95% confidence level (p -value > 0.05) based on a two-tailed Student's t -test.



Supplementary Figure 12. CLM5crop simulated global and national de-trended yield for top five producers of maize, rice, soybean, and wheat when forced by reanalysis climate data relative to FAO reported yield for years 1993-2012. Time series of CLM5crop yield is shifted by one year if the correlation coefficient with FAO reported yield is increased by at least 0.3. R-values indicate Pearson correlation coefficient of CLM5crop vs FAO historical timeseries.



Supplementary Figure 13. CLM5crop simulated global and national yield for top five producers of maize, rice, soybean, and wheat when forced by reanalysis climate data relative to FAO reported yield for years 1993-2012. Time series of CLM5crop yield is shifted by one year if the correlation coefficient with FAO reported yield is increased by at least 0.3. RMSE values indicate root-mean-square error of CLM5crop vs FAO historical timeseries.